Climate Dynamics
https://doi.org/10.1007/s00382-023-07017-w

ORIGINAL ARTICLE

# Storm identification for high-energy wave climates as a tool to improve long-term analysis

**Vincent Kümmerer**[1] · **Óscar Ferreira**[1] · **Valeria Fanti**[1] · **Carlos Loureiro**[1,2]

Received: 2 May 2023 / Accepted: 6 November 2023


## Abstract

Coastal storms can cause erosion and flooding of coastal areas, often accompanied by significant social-economic disruption. As such, storm characterisation is crucial for an improved understanding of storm impacts and thus for coastal management. However, storm definitions are commonly different between authors, and storm thresholds are often selected arbitrarily, with the statistical and meteorological independence between storm events frequently being neglected. In this work, a storm identification algorithm based on statistically defined criteria was developed to identify independent storms in time series of significant wave height for high wave energy environments. This approach proposes a minimum duration between storms determined using the extremal index. The performance of the storm identification algorithm was tested against the commonly used peak-over-threshold. Both approaches were applied to 40 and 70-year-long calibrated wave reanalyses datasets for Western Scotland, where the intense and rapid succession of extratropical storms during the winter makes the identification of independent storm events notably challenging. The storm identification algorithm provides results that are consistent with regional meteorological processes and timescales, allowing to separate independent storms during periods of rapid storm succession, enabling an objective and robust storm characterisation. Identifying storms and their characteristics using the proposed algorithm allowed to determine a statistically significant increasing long-term trend in storm duration, which contributes to the increase in storm wave power in the west of Scotland. The coastal storm identification algorithm is found to be particularly suitable for high-energy, storm-dominated coastal environments, such as those located along the main global extratropical storm tracks.

**Keywords** Coastal storm · Storm independence · Wave reanalysis · Wave power · Northeast Atlantic · Western Scotland

## 1 Introduction

Coastal storms are extreme events characterised by intense hydrodynamic forcing (such as large waves and elevated water levels) leading to beach erosion and coastal flooding, often accompanied by significant social-economic disruption (Harley 2017). In the context of climate change, the risk associated with coastal storms is increasing due to sea-level rise (Melet et al. 2018), projected changes in coastal extreme wave conditions (Bricheno et al. 2023), and expanding coastal populations (Neumann et al. 2015). Consequently, the analysis of storm events is paramount for coastal management. Characterising past storm events allows to identify the climatic controls and trends in storminess parameters, which are needed for strategic adaptation planning and disaster preparedness in coastal areas (e.g., Garnier et al. 2018).

Recent trends and future projections of extreme wave conditions are mostly assessed in global-scale studies (e.g.,

✉ Vincent Kümmerer
vkuemmerer@ualg.pt

Óscar Ferreira
oferreir@ualg.pt

Valeria Fanti
vfanti@ualg.pt

Carlos Loureiro
cloureiro@ualg.pt

[1] Centro de Investigação Marinha e Ambiental (CIMA/ARNET), Universidade do Algarve, Campus de Gambelas, 8005-139 Faro, Portugal

[2] Geological Sciences, School of Agricultural, Earth and Environmental Sciences, University of KwaZulu-Natal, Westville Campus, Durban 4000, South Africa

Published online: 05 December 2023

Young and Ribal 2019; Timmermans et al. 2020; Lobeto et al. 2021; Morim et al. 2021; Sharmar et al. 2021; Erikson et al. 2022). These often outline different results in the magnitude and direction of historical trends because of diverse data, different assessment periods, and methodologies. For example, Sharmar et al. (2021) show differences in annual extreme wave heights (> 95th percentile) of 1.2 m between different reanalysis products for the same assessment period. Furthermore, Erikson et al. (2022) show that trends in the annual number of days where the daily-maximum significant wave height exceeds 6.0 m can be negative or positive for different global wave products for the period between 1980 and 2014. Findings in global scale analyses are restricted to ocean basins and are not directly transferable to the coast because nearshore bathymetry is poorly resolved in global models. Therefore, global-scale studies need to be complemented with higher-resolution regional-scale analysis that can verify and compare ocean-basin trends with coastal areas. For that, locally validated and calibrated wave data and the consideration of regional meteorological processes are important for a robust assessment of changes in storminess. Small changes in the storm climate, at regional and local scale, can significantly enhance coastal erosion. For example, Harley et al. (2017) attributed severe coastal erosion in Southeast Australia to the anomalous storm wave direction of an extratropical cyclone. Similarly, 5° changes in the storm wave direction were found to be a main driver of heightened erosion in Northwest Spain during the winter of 2013/14 (Flor-Blanco et al. 2021). On the West coast of the U.S., changes in the storm wave period can drive large increases in the total water level and consequently storm impacts (Serafin et al. 2019). These examples highlight that detailed assessments of the storm wave climate and its variability are essential for understanding regional coastal impacts.

There are numerous approaches to identify coastal storms depending on data availability and the scope of analysis. In a review of coastal storm definitions, Harley (2017) indicated that coastal storms are created by meteorologically induced disturbances to the local maritime conditions (i.e., waves or water levels) that have the potential to alter the coastline. In contrast to a synoptic climatological approach in assessing coastal storminess that links coastal observations with regional synoptic observations such as storm tracks, statistical based climatological studies of coastal extreme wave occurrences are not able to link every storm to a particular synoptic system. However, a robust storm definition and statistically derived thresholds improve the likelihood of meteorological independence between storms (Harley 2017). Therefore, statistical approaches typically consider a minimum duration threshold between consecutive events to determine meteorological independence between storm events (e.g., Corbella and Stretch 2012; Loureiro and Cooper 2018; Martzikos et al. 2021a; Amarouche et al. 2022). This minimum duration threshold has been designated as meteorological independence criterion (Harley 2017), inter-exceedance time (Fawcett and Walshaw 2008), inter-arrival time (De Michele et al. 2007), or run parameter (Oikonomou et al. 2020). According to the definition of Harley (2017), the minimum duration threshold is linked to the average time interval between the passage of different synoptic systems (e.g., tropical or extra-tropical cyclones) that generate storms and can be used to identify meteorologically independent storm events. Using different values for the duration threshold can substantially influence storm characterisation (Sénéchal et al. 2017; Castelle and Harley 2020) and yet, this parameter is typically selected arbitrarily or neglected in coastal storm analyses (e.g., Senechal et al. 2015; Masselink et al. 2016; Flor-Blanco et al. 2021; Vieira et al. 2021; Celedón et al. 2022).

Most regional to local coastal storm analyses have been performed in low to medium wave energy environments (e.g., Almeida et al. 2011; Mendoza et al. 2011, 2013; Dissanayake et al. 2015; Plomaritis et al. 2015; Garnier et al. 2018; Amarouche et al. 2022; Martzikos et al. 2021b), while only a few were conducted in storm-dominated (Davies, 1980) or high wave energy environments that are common in higher latitudes (e.g., Loureiro and Cooper 2018; Wojtysiak et al. 2018). Low to medium energy wave environments are characterised by mean significant offshore wave heights below 2 m, whereas mean significant wave heights in storm-dominated high energy wave environments are above 2 m (Short 1999). A challenging characteristic in such locations is the frequent temporal clustering of extratropical cyclones (Pinto et al. 2014; Priestley et al. 2017a, b), which further complicates the appropriate estimation of the minimum duration between consecutive storm events. These extratropical cyclone clusters can be generated by meteorological phenomena such as secondary cyclogenesis (Mailier et al. 2006) creating cyclone families (Priestley et al. 2020) or shifts in large-scale atmospheric flow characterised by an intensified jet stream (Dacre and Pinto 2020), resulting in events that are meteorologically related. Other mechanisms can lead to the temporal clustering of storm wave events, challenging the definition of a minimum duration threshold. That was the case of a cut-off-low system that became stationary off the coast of South Africa in 2007, leading to long and intense storms that resulted in dramatic coastal erosion (Smith et al. 2010). The same can occur when tropical cyclones display irregular paths or stall for significant periods such as Hurricane Harvey in 2017 (Hall and Kossin 2019). Therefore, processes taking place in storm-dominated environments challenge existing methods for identifying independent storm events due to the frequent temporal clustering of storms, which may be driven by related meteorological systems.

So far, no generalised storm identification procedure exists for storm-dominated or high wave energy coastal areas, which ultimately affect coastal management planning due to incorrect definition of coastal risks. This work presents a generic storm definition that is adapted to energetic wave climates and considers meteorological independence between storms based on long-term wave statistics. The storm identification algorithm is compared against the common peak-over-threshold storm identification method, with both approaches being applied to two long-term wave reanalysis datasets that have been validated and calibrated with buoy observations. To develop a storm definition suitable for high-energy wave climates this work explores wave data from the Outer Hebrides (west of Scotland) (Fig. 1), located along the North Atlantic storm track and exposed to frequent and intense winter storms. This paper presents a robust approach to identify storms in high wave energy coastal areas and discusses the implications for the analysis of storminess trends and storm climate variability.

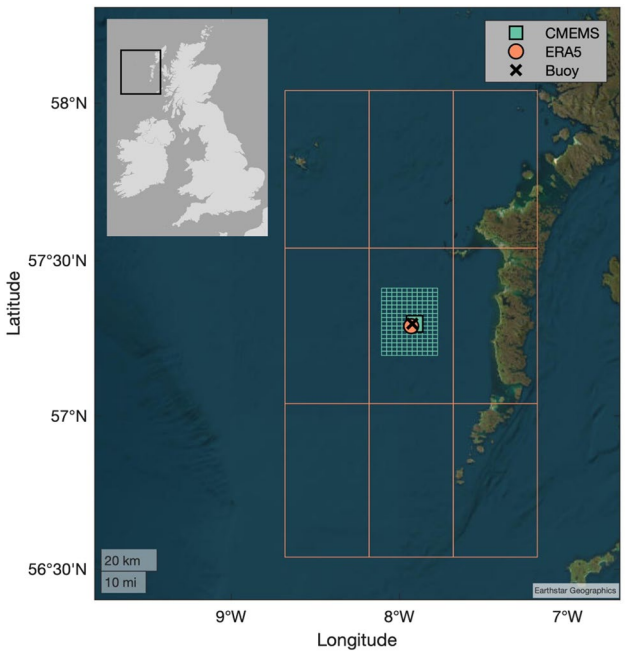


**Fig. 1** Location of the Outer Hebrides, West Scotland, wave reanalysis grid outlines (ERA5 in orange and CMEMS in green), and data output locations

## 2 Data and methodology

### 2.1 Wave data

Significant wave height ($H_s$) and peak wave period ($T_p$) datasets from the Outer Hebrides were used to demonstrate the storm identification approach and for presenting an application example of storm characterisation in a high wave energy coastal environment. While buoy observations are available for the last 11 years (Table 1), two recent and state-of-the-art reanalysis products were used to provide a continuous and extended wave time series, as well as to enable a comparison between widely used wave model products. However, when compared to in-situ observations wave reanalyses can exhibit systematic errors, such as under or over-estimation of extreme wave heights (Baordo et al. 2020). Hence, when analysing extreme events from wave reanalyses, it is paramount to correct these systematic errors by applying calibration functions obtained from the comparison with buoy data (Fanti et al. 2023). Moreover, different reanalysis products can yield differences in the magnitude and direction of long-term trends (Timmermans et al. 2020; Sharmar et al. 2021), which highlights the importance of performing a multisource analysis (Erikson et al. 2022).

For this work, wave buoy observations were obtained from the West of Hebrides buoy, deployed and operated by CEFAS aproximately 30 km offshore the Outer Hebrides in the west of Scotland (Fig. 1) in a water depth of 100 m. Wave parameters and spectra are recorded for periods of 30 min using a Datawell Directional Waverider MkIII buoy. The modelled wave data used in this work were obtained from the ERA5 reanalysis (Hersbach et al., 2020; Bell et al. 2021), provided by the European Centre for Medium-Range Weather Forecasts, and the Northwest European Shelf Wave Hindcast, provided by the Copernicus Marine Service (hereafter CMEMS). ERA5 covers seven decades (1951–2020) with hourly data and a 0.5° × 0.5° spatial resolution, while CMEMS is restricted to four decades (1980–2020), with data every 3 h and a 0.017° × 0.017° resolution (Table1).

**Table 1** Synthesis of the wave data used and designation of the datasets

| | Coordinates | Sampling Interval | Period | Variables | Source | Dataset designation |
|---|---|---|---|---|---|---|
| Buoy | 57.289° N, – 7.923° W | 0.5 h | 2009–2020 | Hs, Tp | CEFAS | Buoy-11 |
| ERA5 | 57.29° N, – 7.93° W | 1 h | 1950–2020 | Hs, Tp | ECWMF | ERA5-11; ERA5-40; ERA5-70; cERA5-11; cERA5-40; cERA5-70 |
| CMEMS | 57.2973° N, – 7.9091° W | 3 h | 1980–2020 | Hs, Tp | Copernicus Marine Service | CMEMS-11; CMEMS-40; cCMEMs-11; cCMEMS-40 |

ERA5 and CMEMS wave data were extracted for the closest point to the Outer Hebrides wave buoy (Fig. 1). More information on the buoy and the reanalyses data and their validation against buoy observations are provided in the supplementary materials.

The observations from the Outer Hebrides wave buoy were used for validation and calibration of the two wave reanalyses. The calibration focused on the extreme values (> 95th percentile) of Hs, $T_m$, and $T_p$, and transfer functions with best fits were applied to the model data (y) to better reproduce the buoy observation (x). Several transfer functions were tested, including linear, quadratic, and power functions, as well as a rotation around the mean following Fanti et al. (2023). The transfer functions used for $H_s$ and $T_m$ are a power function (Eq. 1), while for $T_p$ a rotational function around the mean was applied (Eq. 2) which is derived from the rotational matrix in Eq. 3.

$$y' = ay^b, \tag{1}$$

$$y' = sin\beta\left(x - x_c\right) + cos\beta\left(y - y_c\right), with\beta = (1 - a), \tag{2}$$

$$\begin{bmatrix} x' \\ y' \end{bmatrix} = \begin{bmatrix} \cos(1-a) & -\sin(1-a) \\ \sin(1-a) & \cos(1-a) \end{bmatrix} \begin{bmatrix} x - x_c \\ y - y_c \end{bmatrix}, \tag{3}$$

The transfer functions were then applied to the long-term data set (i.e., the 70 and 40 years) assuming that deviations in the reanalysis relative to the buoy data are consistent for the entire analysis period.This resulted in the calibrated ERA5 and calibrated CMEMS wave time series and, as such, the long-term data sets are referred to as cCMEMS-40, cERA5-40, and cERA5-70, where "c" stands for calibrated and the numbers refer to the length of the analysis period, specifically 70 years (1950–2020), 40 years (1980–2020), and 11 years for the buoy data (2009–2020).

Similarly to previous studies on the wave climate of the Northeast Atlantic (e.g., Santo et al. 2015), here the winter season is defined as the extended boreal winter comprising the months of October to March (ONDJFM). The ONDJFM extended winter considered here is also consistent with the time period when most extreme sea-level events occur in the northwest of the UK (Haigh et al. 2016). For simplicity, the winter year designation used in this work refers to the second part (JFM) of the winter season, meaning that winter 2020 refers to OND of 2019 and JFM of 2020.

## 2.2 Storm identification

There are many coastal storm identification approaches based on time series, which use variables such as Hs, Tp, wave direction, and water levels (Martzikos et al. 2021a and references therein). Storm identification can be based on single, combined, or composite parameters (e.g., storm power), but the most common approaches rely on $H_s$ time series (Harley 2017). However, the identification of storms from $H_s$ time series lacks a consistent methodology, as recently outlined by Harley (2017) and Martzikos et al. (2021a). Existing definitions of coastal storm events (based on $H_s$ data) encompass several concepts, criteria, and thresholds, and are often topic specific. In storm erosion studies for example, the $H_s$ thresholds are based on hydrodynamic conditions that result in significant morphological change (e.g., Almeida et al. 2012; Armaroli et al. 2012; Del Río et al. 2012), and the duration thresholds are based on the subsequent morphological recovery periods (e.g., Loureiro et al. 2012; Senechal et al. 2015). Consequently, storm criteria and thresholds become highly site-specific due to the varying coastal morphodynamics, wave climate characteristics and regional meteorological systems that generate the storms (Ciavola et al. 2014; Harley 2017). Because of this, Castelle and Harley (2020) encourage generic criteria for storm identification based on long-term wave statistics, as this allows to broaden the application and compare findings from coastal storm analyses.

### 2.2.1 Conceptual description

Typically, the identification of storm events for climatic analysis of storminess considers three criteria: (1) an extreme $H_s$ threshold, hereafter storm threshold (ST), (2) a minimum storm duration (MSD), and (3) an independence duration (ID) (Ciavola et al. 2014; Harley 2017; Martzikos et al. 2021a). However, these three storm identification criteria have been mostly applied in low to medium-energy wave environments. In storm-dominated or high wave energy environments with consecutive and rapidly succeeding storms, an additional criterion needs to be considered to ensure appropriate aggregation or separation between consecutive exceedances of the $H_s$ storm threshold. The proposed criterion is designated as the independence threshold (IT). These four storm identification criteria are explained conceptually below and defined statistically in Sect. 2.2.2.

The ST determines if wave conditions are considered extreme and hence separates the $H_s$ time series into storm ($H_s$ > ST) and calm periods ($H_s$ < ST). In the simpler situation (Fig. 2, S1), when ST is up-crossed, it dictates the start of a storm, and likewise, when it is down-crossed it defines the end of a storm.

During storms, waves can temporarily down-cross the storm threshold, but this does not necessarily imply that a storm has ended, and as such it is necessary to also consider the length of time between successive down-crossings and up-crossings of ST. This is defined as the Independence Duration (ID) and is used to determine the meteorological and statistical independence between consecutive storm

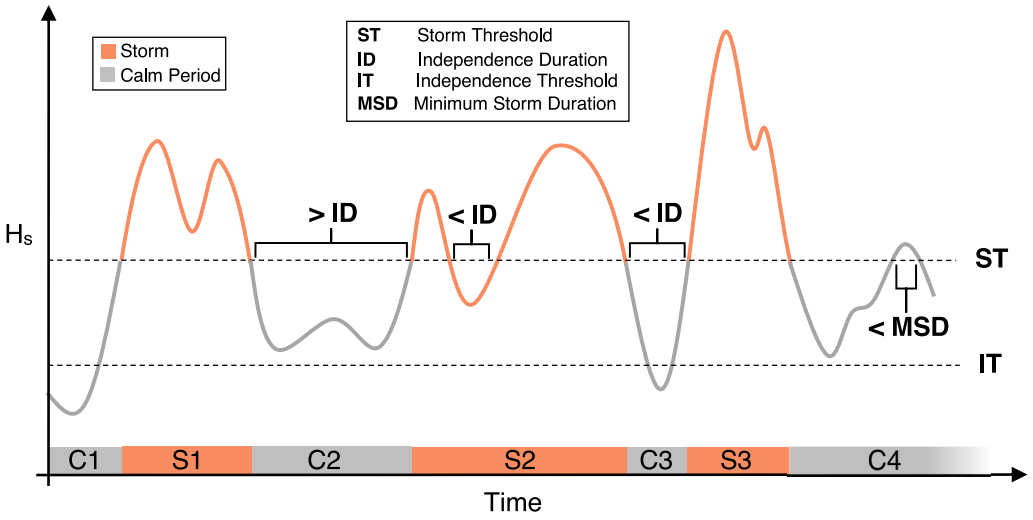


**Fig. 2** Synthetic representation of the storm identification methodology adapted to high wave energy environments. $H_s$ is the significant wave height. C1–C4 are the calm periods between storms, and S1–S3 are individual storm events

events, by combining exceedances of ST into one storm event until the inter-exceedance period is long enough to assume independence. In a meteorological or oceanographic context, ID corresponds to the average passage time of synoptic systems that drive storms over a coastal area (e.g., Harley 2017). From a statistical perspective, a storm analysis should be conducted on an independent (and identically) distributed extreme value dataset (e.g., Lopatoukhin et al. 2000). The extreme value dataset usually consists of an extreme wave height, period, or power for each independent storm, which is then used for further statistical analysis. However, a single storm can include several $H_s$ peaks with occasional periods of $H_s < ST$. Consequently, an independent storm is only considered when the period between a down-crossing of ST and the following up-crossing is longer than ID (Fig. 2, C2), and when the duration between consecutive up-crossings is shorter than ID the storm is extended in time (Fig. 2, S2).

This approach enables brief crossings below ST within a single storm event by combining several $H_s$ peaks in rapid succession that belong to the same meteorological disturbance (Harley 2017).

However, periods of rapid storm succession that are common in storm-dominated coasts in the winter season can lead to storms lasting several weeks, which are likely caused by different meteorological disturbances. Therefore, to enhance meteorological independence an additional independence threshold (IT) is defined. IT is a $H_s$ threshold that represents storm dissipation. Consequently, IT must be smaller than ST but above the mean $H_s$ for the coastal region. In the case of rapid storm succession (Fig. 2, S2, S3), when the time between two consecutive storms is shorter than ID but $Hs < IT$ (Fig. 2, C3), two independent storm events should be considered (Fig. 2, S2 and S3). By including IT in the storm identification, the independence between consecutive storms can be achieved in two ways: if after a down-crossing Hs remain below ST for longer than ID (Fig. 2, C2), or if Hs falls below IT (Fig. 2, C3).

Finally, not all records that exceed ST should be considered a storm, as storm events must have a minimum duration. Therefore, when storm duration is lower than the MSD, the event is not considered a storm (Fig. 2, C4). The role of MSD is to filter out short-lived exceedances of ST that will have no relevant impacts on the coast (Martzikos et al. 2021a).

The performance of the proposed storm identification approach was tested against a simple Peak-Over-Threshold (POT) approach which is still widely used for the characterisation of coastal storms (e.g., Flor-Blanco et al. 2021; Vieira et al. 2021; Celedón et al. 2022; Gramcianinov et al. 2023b). In extreme value analysis, the POT approach refers to the extraction of peak $H_s$ values from threshold exceedance clusters (e.g., Ferreira and Guedes Soares 1998), whereas in coastal storm analysis the POT approach can also refer to the extraction of all threshold exceedances of the cluster to analyse storm characteristics such as duration and power (Harley 2017). A simple POT approach considers ST as a stand-alone storm criterion, with each storm identified as the consecutive wave records over the ST (e.g., Weisse and Gunther 2007; Gramcianinov et al. 2023b), but neglects MSD, ID and IT. In the example of Fig. 2, storm S2 would be identified as two separate storms by the POT approach because no independence duration is defined. In addition, considering the POT approach, the $H_s$ peak in C4 would be identified as an additional storm. Differences between the proposed storm identification and the POT approach were

assessed by comparing the long-term storminess metrics using the Outer Hebrides datasets as a case study (Sect. 2.4). Additionally, a sensitivity analysis of the storm criteria was performed by attributing changes in the total storm counts and storm duration to each storm criterion, given that both storm count and duration have been shown to be sensitive to changes in storm identification methods (Sénéchal et al. 2017; Castelle and Harley 2020).

#### 2.2.2 Statistical definition

The two $H_s$ thresholds, ST and IT, are estimated based on long-term $H_s$ records. In line with most coastal storm analyses (e.g., Masselink et al. 2014; Castelle et al. 2015; Harley et al. 2017; Martzikos et al. 2021b), ST was defined as the 95$^{th}$ percentile of the $H_s$ time series. IT aims to determine the conditions below which $H_s$ is no longer associated with a storm event by considering the average conditions of the season with most storm occurrences. Based on this, IT is defined as the mean winter $H_s$, as it will be lower than ST but higher than the long-term mean $H_s$ for the coastal region.

The selection of an appropriate ID is more challenging as it requires consideration of the average passage time of a meteorological or oceanographic system driving the storm (Harley 2017). As a consequence, ID is commonly selected arbitrarily in coastal storm analyses. However, ID can be estimated statistically based on the extremal index proposed by Ferro and Segers (2003). This approach has been used previously in the estimation of return periods of extreme $H_s$ occurrences (Oikonomou et al. 2020), extreme precipitation (Barton et al. 2016) and extreme water levels (Arns et al 2013).

For the calculation of the extremal index, a binary parameter $W_i$ is defined so that $W_i = 1$ when $H_s > ST$ and $W_i = 0$ when $H_s < ST$, similarly to the POT approach. The total count of independent storms, Z, is given by

$$Z = \sum_{i=1}^{n} W_i\left(1 - W_{i+1}\right) \ldots \left(1 - W_{ID+1}\right), \tag{4}$$

where n is the number of $H_s$ data points (Smith and Weissman 1994). Ferro and Segers (2003) demonstrate that the extremal index ($\theta, \in [0, 1]$) describes the proportion of non-zero inter-exceedance times of an extreme event and the reciprocal of the mean of the non-zero inter-exceedance times as demonstrated by Smith and Weissman (1994). Therefore, θ can be defined as

$$\theta(ST) = \frac{2\left[\sum_{j=1}^{N-1}\left(T_j - 1\right)\right]^2}{(N-1)\sum_{j=1}^{N-1}(T_j - 1)\left(T_j - 2\right)}, \tag{5}$$

where $T_j$ is the time between two consecutive ST exceedances with $j \in [1, N-1]$ and $T_j > 2$, and as an estimate of the true extremal index:

$$\theta' = Z/N, \tag{6}$$

corresponding to the reciprocal of the mean storm duration, where N is the number of total ST exceedances:

$$N = \sum_{i=1}^{n} W_i \tag{7}$$

After calculating θ (Eq. 5) it is possible to estimate Z (Eq. 6) iteratively through Eq. 4, increasing ID values until Z is reached. ID is therefore estimated based on the $H_s$ time series itself and explained by asymptotic theory (Ferro and Segers 2003). When seasonality in the extreme wave climate is expected, the long intervals between consecutive storms during the calm or summer season contribute to the overestimation of ID (Oikonomou et al. 2020). Therefore, for the calculation of ID, the $H_s$ time series is restricted to the winter season, when most extreme value exceedances occur.

The MSD was set to 6 h, which is a commonly used minimum duration for coastal storm analysis (Martzikos et al. 2021a and references therein). This MSD value assumes that storms that last at least 6 h have a high-likelihood (~70%) of coinciding with high-tide conditions in a semi-diurnal tidal cycle, which increases the possibility of significant storm-induced morphological impacts on the coast and minimizes the loss of extreme wave records in the storm analysis. Furthermore, the 6 h MSD ensures that a minimum of 2 storm records are used for storm identification using the CMEMS reanalysis, as this has the lowest temporal resolution (3 h) of the datasets considered (Table 1).

### 2.3 Long-term analysis

Following the application of the storm identification algorithm, storm parameters were estimated to define and characterise each storm event and compute aggregated winter metrics. The storm duration describes the time between the start and end of an independent storm (Fig. 2, S1-3), and accounts for the sampling intervals of the different wave records (Table 1). For the characterisation of each independent storm event, mean storm $H_s$ ($SH_s$), mean storm $T_p$ ($ST_p$), and the 98th percentile of $SH_s$ and $ST_p$ were computed. In order to compare averaged wave trends with other studies, the winter mean and 98$^{th}$ percentile of $H_s$ and $T_p$ were computed in addition to storm metrics. The storm power (SP) was calculated following Splinter et al. (2014), with

$$SP = \int_0^D \frac{\rho g^2}{64\pi} SH_s^2 ST_p \Delta t, \tag{8}$$

where D is the storm duration, ρ is the seawater density (~ 1024.5 kg/m$^3$), g is the gravitational acceleration (9.81 m/s$^2$), and Δt is the sampling interval.

The maximum $H_s$ value of each identified winter storm was used to form an independent and identically distributed extreme value dataset and was used to determine the return period of extreme $H_s$ conditions. However, using the POT approach that lacks the ID criteria to identify storms could violate the independence requirement for the extreme value dataset. The return periods of $H_s$ were estimated from 1 to 100 years by fitting the Generalized Pareto Distributions (GPD) to the winter storms $H_s$ datasets, and assuming stationarity (e.g., Coles 2001). To meet the homogeneity requirement for the application of extreme value theory, only the storms during the ONDJFM season were considered. The GPD was fitted via numerical maximum-likelihood estimation, with return periods of maximum $SH_s$ ($RSH_s$) values defined by:

$$RSH_s = TH + \frac{\sigma}{\xi}\left[\left(\frac{RL}{\lambda}\right)^{\xi} - 1\right] \text{for} \xi \neq 0 \quad (9)$$

where σ is the scale parameter of the GPD, ξ is the shape parameter of the GPD, R is the return period, L is the length of the extreme value dataset, and λ is the period of the $H_s$ time series in years. Calculating $H_s$ return periods for the various datasets considered in this work (Table 1), including the buoy and the calibrated reanalysis data, provides additional validation of the calibration as it allows to consider the results for the higher percentiles of the $H_s$ data (Fanti et al. 2023).

Winter storm counts and storm parameters were calculated to analyse the variability and periodicity of storminess in the Outer Hebrides and to compare the proposed storm identification algorithm and the common POT approach. The significance of the long-term trends was determined using the Mann–Kendall test and the magnitude and direction of the trends were estimated using Sen's slope, following Young and Ribal (2019) and Erikson et al. (2022), as this provides robust trend estimates when data are non-normally distributed. The significance of long-term trends was tested considering 0.05 and 0.1 significance levels. Climatic control of winter storminess was explored through correlation analysis of the storm parameters with the North Atlantic Oscillation (NAO) index, which is the leading mode of climate variability in the NE Atlantic (e.g., Hurrell 1995; Scott et al. 2021). To determine the extended winter NAO, sea level pressure data were obtained from the National Centre for Atmospheric Research (NCAR) for Lisbon (40.0N, 10.0W) and Reykjavik (65.0N, 20.0W) and used to compute the station-based NAO. The NAO was computed using a reference period from 1951 to 1980 and normalized to monthly sea level pressure following the method proposed by the Climate Research Unit (2022) for station-based NAO index estimation. For consistency with the storm analysis, the NAO index was calculated for the extended winter season (ONDJFM). The correlation between the extended winter NAO and winter storm parameters was computed with Pearson's linear correlation coefficient (R) considering a 0.05 significance level.

### 2.4 Study site

The wave climate of the Outer Hebrides (Fig. 1) is considered one of the most energetic globally, with a fetch of more than 6000 km for the dominant W to WNW wave direction (Ramsay and Brampton 2000). Consequently, the Outer Hebrides have been the focus of wave energy extraction research due to the high wave power resources (e.g., Neill et al. 2017). The wave climate of the west of Scotland displays high seasonality, with very energetic conditions throughout the extended winter season from October until the end of March (Santo et al. 2015). The winter wave climate in this region is also highly correlated with the NAO, where a positive NAO index is associated with energetic winters and a negative or lower NAO index with calmer winter conditions (Santo et al. 2015; Castelle et al. 2017; Hochet et al. 2021; Scott et al. 2021). The well-established association between positive NAO and increased winter storminess determined from wind records was linked to increasing coastal erosion in the Outer Hebrides (Dawson et al. 2004). Dawson et al. (2007) argue that winter storminess in the west of Scotland was lower in the first part of the twentieth century compared to the late nineteenth century, as evidenced by mean monthly wind velocities and monthly maximum gust velocities. Santo et al. (2015) demonstrated that offshore the Orkney islands, in the north of Scotland, the wave power climate was characterised by strong interannual and multidecadal variability between 1665 and 2005. Furthermore, extreme $H_s$ (Castelle et al. 2018) and wave storminess (Loureiro and Cooper 2018) have been shown to exhibit a positive long-term linear trend since 1950 in the higher latitudes of the NE Atlantic. Therefore, the intensity, frequency, and variability of storms in the Outer Hebrides make this area an ideal location to develop and test a robust storm identification for high-energy or storm-dominated environments as a basis for analysing storminess patterns.

## 3 Results

### 3.1 Reanalysis calibration

ERA5-11 and CMEMS-11 data for $H_s$ and $T_p$ show an overall good performance when compared to the Outer Hebrides buoy observations, although CMEMS-11

outperforms ERA5-11 in most error metrics (Fig. SM1). The highest correlation coefficients (R = 0.98) were found for $H_s$ in both ERA5-11 and CMEMS-11. However, both wave models show negative biases for $H_s$ and $T_p$ indicating a systematic underestimation particularly evident for the extreme wave conditions (Fig. SM1). For example, in the most extreme event on record, which occurred on the 1st of February 2016, the buoy records a maximum $H_s$ = 16.4 m, while the modelled values of $H_s$ were 14.1 m and 13.9 m for ERA5-11 and CMEMS-11, respectively. The calibration applied to the reanalysis datasets aimed to reduce the systematic underestimation, resulting in a bias improvement in $H_s$ of 0.24 m and 0.09 m for cERA5-11 and cCMEMS-11, respectively (Fig. 3a, b).

The calibration also improved the Root Mean Square Error (RMSE) and the Scatter Index (SI) for $H_s$ and $T_p$ in both ERA5 and CMEMS (Fig. 3). While after calibration the cCMEMS-11 dataset statistically outperforms cERA5-11, it is apparent that $H_s$ values above 12 m are better estimated in cERA5-11, as these remain underestimated in cCMEMS-11 (Fig. 3a, b). The calibration also improves the agreement between model data and buoy observations for $T_p$, including extreme $T_p$ values. As with $H_s$, cCMEMS-11 also outperforms cERA5-11 in terms of error metrics for $T_p$ (Fig. 3c, d).

### 3.2 Storm identification criteria

The storm criteria ST, ID, and IT vary according to the dataset and the corresponding analysis period (Table 2).

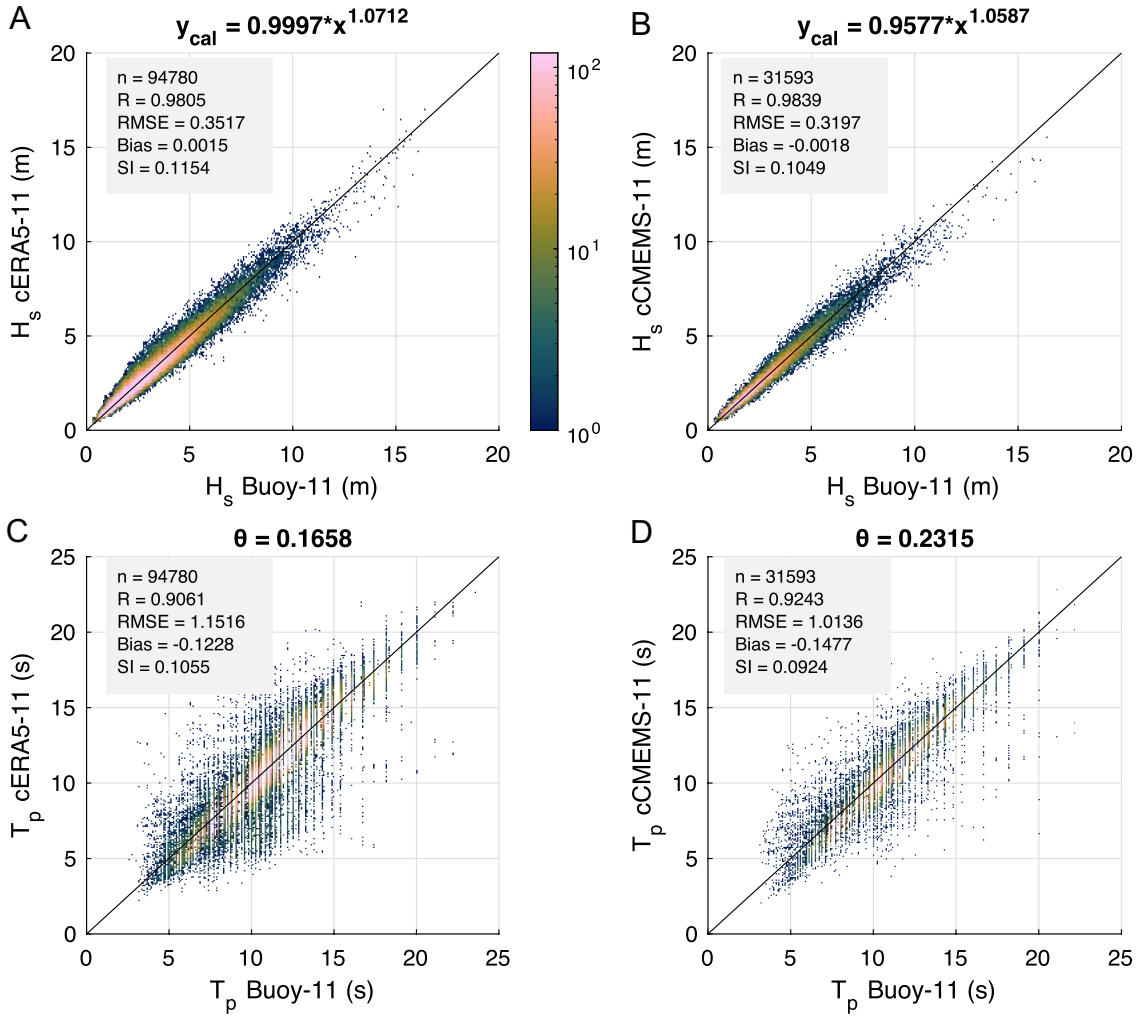


**Fig. 3** Density scatter plots of calibrated model $H_s$ (**A**, **B**) and $T_p$ (**C**, **D**) against buoy measurements, with the transfer function (A, B), and angle of rotation (**C**, **D**) used for calibration. The inset boxes show the number of records (n), the correlation coefficient (R), the Root Mean Squared Error (RMSE), the bias, and the scatter index (SI). Note that the CMEMS reanalysis as a temporal resolution of 3 h, which results in fewer records compared to ERA5 that has a 1-h resolution. The density colorbar in A is representative for all subplots. For more details on the transfer functions and the statistical parameters see the supplementary material

**Table 2** Storm identification criteria for the Outer Hebrides based on the original and calibrated reanalysis datasets

| | Dataset | ST (m) | ID (hours) | IT (m) |
|---|---|---|---|---|
| Original | ERA5-70 | 5.59 | 48 | 3.45 |
| | ERA5-40 | 5.74 | 59 | 3.57 |
| | CMEMS-40 | 6.13 | 54 | 3.73 |
| Calibrated | cERA5-70 | 6.31 | 48 | 3.80 |
| | cERA5-40 | 6.50 | 59 | 3.94 |
| | cCMEMS-40 | 6.53 | 54 | 3.89 |

Moreover, $H_s$ values for ST and IT also increase between the original and calibrated reanalysis data, while ID estimates are not affected by the calibration. Relative to the original datasets, the increase in ST is lower for cCMEMS (0.40 m) than for cERA5 (0.73 m on average for the two analysis periods). Likewise, IT also increases after calibration but more moderately, and differences in ST and IT between cERA5-40, cERA5-70 and cCMEMS-40 are reduced to less than 0.25 m.

Considering the different analysis periods, the cERA5-70 dataset yields ~ 0.2 m lower ST and ~ 0.1 m lower IT estimates than either of the 40-year datasets. A similar pattern is observed in ID, which is higher for cERA5-40 and cCMEMS-40 with 59 h and 54 h, respectively, compared to 48 h for the cERA5-70 dataset. In summary, the calibration reduced the differences in the storm identification criteria between the two reanalyses datasets, with the length of the analysis period (70 or 40 years) leading to a more significant variation in ST, ID, and IT.

As a result of the different storm definition, based on the 70-year period (cERA5-70), the total storm count is reduced from 1653 storms using the POT approach to 941 storms (43% reduction) using the storm identification algorithm (Fig. 4A). The vast majority of the reduction is associated with the inclusion of ID which merges $H_s$ exceedance clusters in close temporal proximity into a single storm. Contrary to counts, duration is increased using the storm identification algorithm compared to using the POT approach (Fig. 4B). The total storm duration in the 70-year $H_s$ dataset using the POT is 1278 days (5% of the time series length, ST is set to the 95th percentile of $H_s$) and 1650 days when using the storm identification algorithm (6.45% of the time series length). Thus, the implementation of the storm criteria ID, IT, and MSD increases the overall storm duration by 29%. This pattern of change between the POT and the storm identification algorithm is also evident in the storm count and duration for the cERA5-40 and cCMEMS-40 datasets. It evidences that storm counts and duration strongly depend on the storm identification criteria used, with ID having the largest influence on total storm metrics, while the contribution of IT and MSD is much lower.

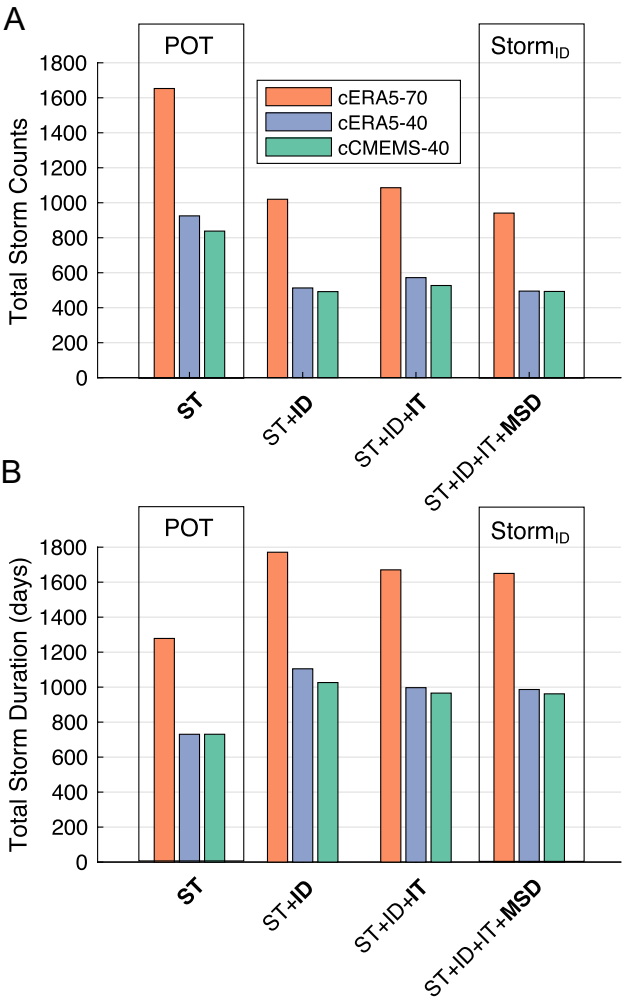


**Fig. 4** Influence of storm criteria on the total storm count (**A**) and storm duration (**B**). Each bar group represents the progression of the storm identification algorithm (Storm$_{ID}$) by introducing an additional storm criterion highlighted in bold. *ST* storm threshold, *ID* independence duration, *IT* independence threshold, and *MSD* minimum storm duration

A period with a rapid succession of storms between December 1992 and February 1993 illustrates the performance of the storm identification algorithm as well as the differences to the POT approach (Fig. 5A). In this example, the storm criteria were estimated based on the cERA5-70 data, with storms identified when $H_s$ exceeds 6.31 m (ST) for a minimum of 6 h (MSD) (Fig. 5A). The first exceedance of $H_s$ (10/12/1992) is not identified by the storm identification algorithm because MSD is less than 6 h.

The following storm (14/12/1992) is identified and characterised identically by the storm identification algorithm and the POT approach because $H_s$ is below ST until the next storm (17/12/1992), which is longer than the ID of 48 h. Major discrepancies between the two storm identification methods occur between 02/01/1993 and 18/01/1993,

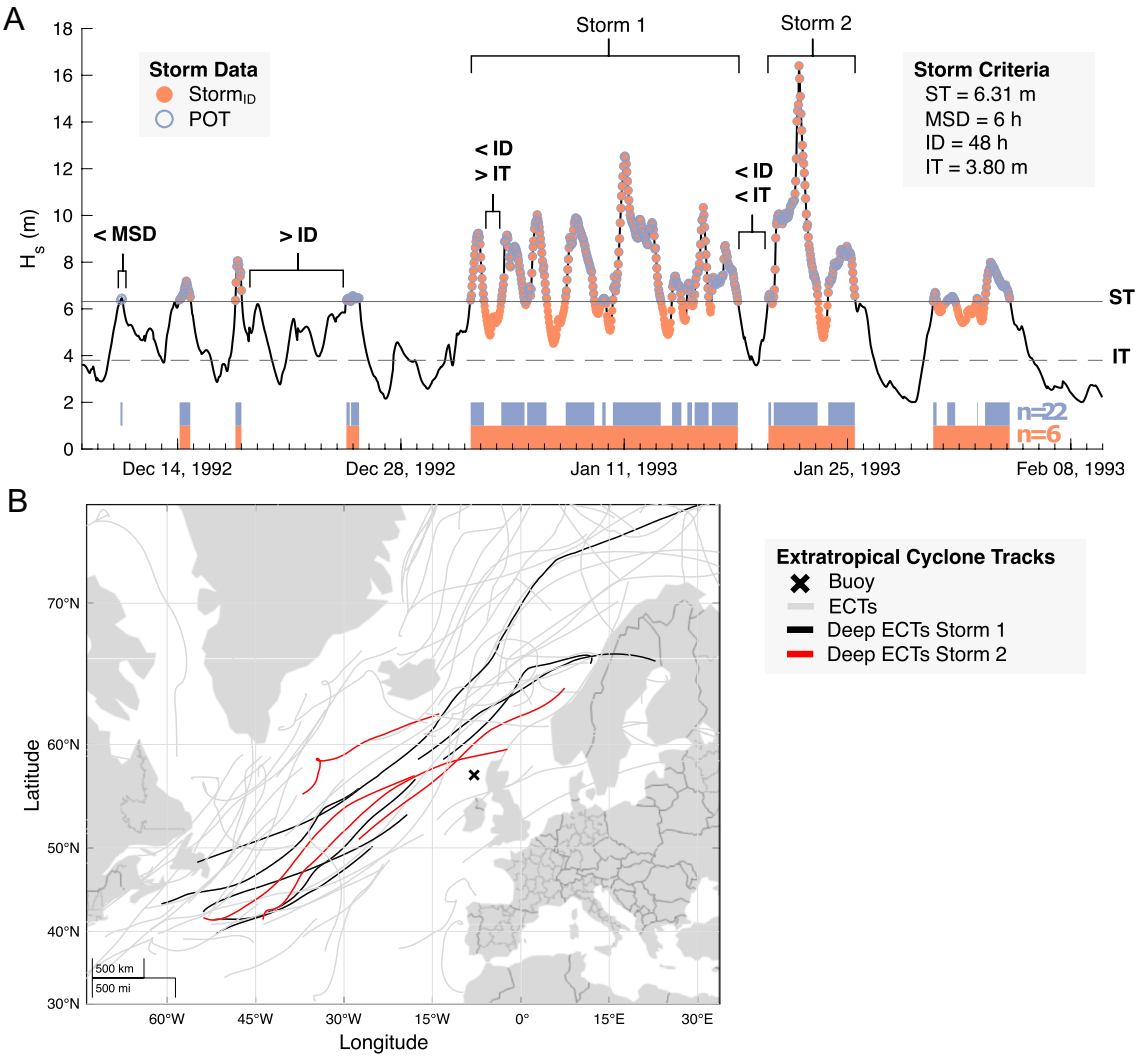


**Fig. 5** **A** Illustration of the storm identification algorithm (Storm$_{ID}$) adapted to high wave energy environments (**A**). The four thresholds embedded in the storm identification algorithm are illustrated on an example period from the cERA5-70 $H_s$ data. The blue rectangles indicate the storm events determined using the POT approach (n = 22) and the orange rectangles when using Storm$_{ID}$ (n = 6). *ST* storm threshold, *MSD* minimum storm duration, *ID* independence duration, *IT* independence threshold. **B** All extratropical cyclones tracks (ECTs) that occurred in the North Atlantic during the period considered in A obtained from Lodise et al. (2022), highlighting the deep extratropical cyclones (minimum pressure below 980 hPa along the track) that occurred during Storm 1 and Storm 2 in A

when $H_s$ varies considerably but remains high throughout the 16 day period. While the POT approach individualises 10 storms for this period, the storm identification algorithm identifies this period as one storm because $H_s$ is never below IT and ID is never exceeded. In fact, this was the most powerful storm since 1950 in the Outer Hebrides based on the storm identification algorithm and cERA5-70 data. This also demonstrates that during a storm event, $H_s$ can fall below ST for considerable periods of time. Through the implementation of IT, this storm ends on 18/01/1994 instead of being extended until 26/01/1993. This occurs because $H_s$ down-crosses IT on 19/02/1993, although the duration between ST exceedances is always below ID. This period of rapid storm succession is reflected by the number and path of extratropical cyclones in the North Atlantic during the same period (Fig. 5B). During the high-energy period (02/12/1992–26/01/1993), there is a sequence of deep extratropical cyclones with similar track orientations. The stacked cyclone tracks suggest the occurrence of serial clustering of extratropical cyclones (Dacre and Pinto 2020), which is likely to be caused by secondary cyclogenesis. The resulting family of extratropical cyclones drives a prolonged period of $H_s$ higher than ST, with occasional short-lived down-crossings, but can be interpreted as a single storm event, with high-energy wave conditions continuously impacting the coastal area.

### 3.3 Storm analysis

According to the cERA5-70 data, 87% of the total storms in the Outer Hebrides occur during the extended winter season (Fig. SM2) with an average of 12 storms per winter. The winter month with the highest total storm occurrence is December with 19% followed by January (16%) and February (14%). The average storm conditions are characterised by $SH_s = 7.21$ m ($SH_s^{98} = 11.21$ m) and $ST_p = 14.10$ s with a dominant westerly direction. Storms last on average 42 h, with a mean storm power of 15.84 $MWhm^{-1}$. The most powerful storms since 1950 were recorded in January of 1993 and 1994, with total storm powers above 162 $MWhm^{-1}$ and storm duration in excess of 2 weeks (Table SM1). The 'Great Storm' of January 2005 (e.g., Dawson et al., 2007) is recorded as the third most powerful storm since 1950 but has the second longest duration (16 days) and $SH_s^{98}$ of 14.8 m, which is over 1 m higher than the storms in January 1993 and 1994.

In terms of return periods of extreme wave conditions, these are underestimated by more than 3 m for the 50 and 100-yr Hs return periods based on uncalibrated wave reanalyses (ERA5-11 and CMEMS-11) in comparision to the buoy data, but improve substantially following calibration (Fig. 6A). While cERA5-11 $H_s$ return periods are similar to those determined with the buoy data, $H_s$ return periods based on cCMEMS-11 data remain underestimaned by more than 1.5 m for return periods > 20 years. The 40 and 70-year reanalysis $H_s$ datasets show a similar pattern in the correction after calibration, yielding slightly lower $H_s$ return periods to those determined with the 11-year dataset (Fig. 6B). There is only a minor difference between the 70-year and 40-year datasets in terms of $H_s$ return periods. In the case of cERA5-40 and cERA5-70, the 100-year $H_s$ return period is 17.28 m and 16.85 m, respectively, while based on the cCMEMS-40 $H_s$ dataset it is 15.12 m. Return values based on the POT approach were not displayed because the $H_s$ return periods are unrealistic high, which is considered to be due to the violation of the statistical independence requirement for the extreme value dataset.

Winter storm counts, cumulative storm duration and power show clear multiannual variability and are remarkably consistent across datasets (Fig. 7). There are, however, differences between the storm identification approaches. The storm identification algorithm produces a lower winter storm count compared to the POT approach, while for the latter total storm duration and storm power are lower (Fig. 7). Despite the differences in value for the different storm metrics, the temporal variability in winter storminess is similar between both approaches. However, storm count variability determined with the POT approach is more pronounced, while variability in storm duration and power are slightly suppressed in the POT compared to the storm identification algorithm.

Considering specifically the winter storminess metrics in the Outer Hebrides determined using the cERA5-70 data and the storm identification algorithm proposed in this work, the winter storm counts range between a minimum of 3 storms (2013) and a maximum of 19 storms (1983 and 1992). Cumulative storm duration over the extended winter season ranges from a total of 106 h in 2001 to 1243 h in 2015, which corresponds to the least and most energetic winters with 38 $MWhm^{-1}$ and 502 $MWhm^{-1}$, respectively.

In general, the storm wave climate in Western Scotland is characterised by a high multiannual variability. Compared to winter storm duration and storm power, the storm counts according to the storm identification algorithm are less variable throughout the studied period. In the early 1990's, there

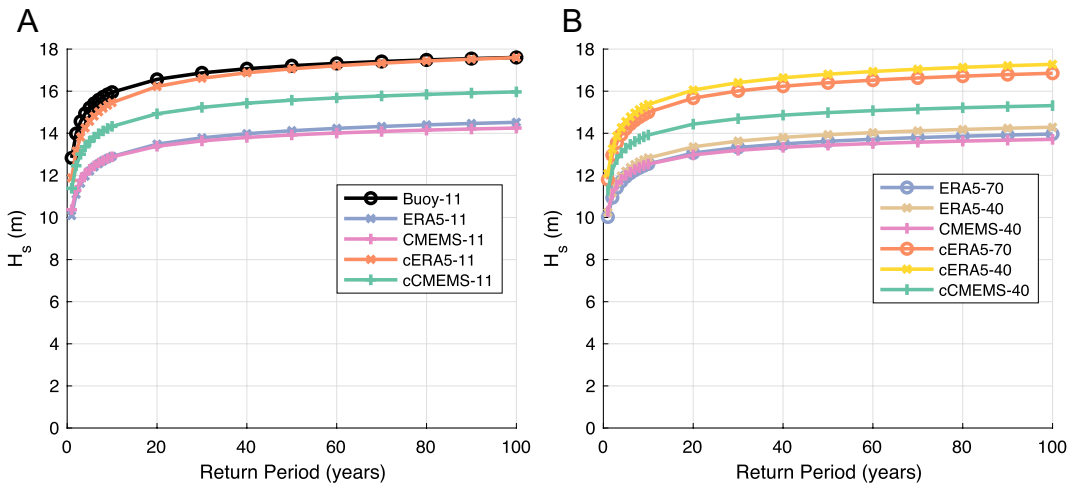


**Fig. 6** $H_s$ return periods for the various datasets. **A** Return period for the buoy and the calibrated/uncalibrated wave models using the reference time of the buoy record (11 years)). **B** Return periods for the calibrated datasets with extended analysis periods (40 and 70 years)

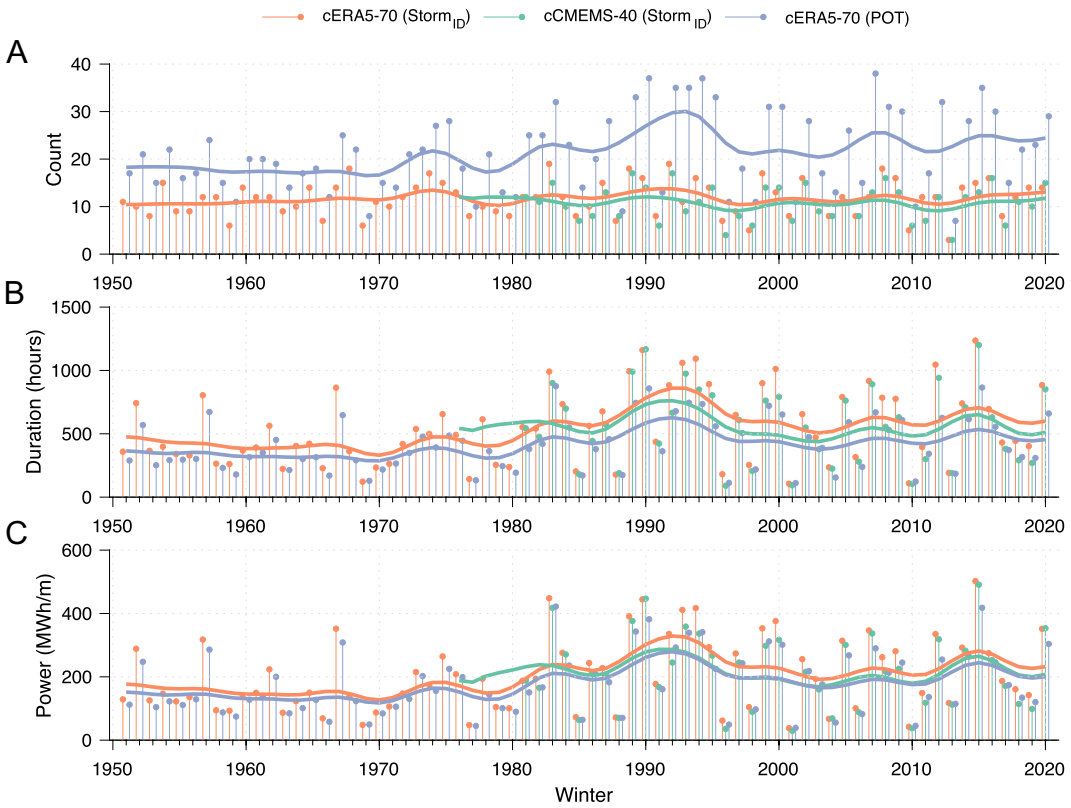


**Fig. 7** Temporal variability in winter storm count (**A**), cumulative storm duration (**B**), and cumulative storm power (**C**) based on two different storm data sets (cERA5-70 and cCMEMS-40) and using the storm identification algorithm and the POT approach (only for cERA5-70). Decadal moving average is indicated by thick lines

is a cluster of energetic winters evidenced by the maximum in the decadal moving average of the winter storm power with ~ 330 $MWhm^{-1}$ and winter storm duration with ~ 750 h. Aside from a few energetic winters, the period between 1950 and 1980 is less energetic when compared to the period from 1980 to 2020.

The cumulative winter storm duration and power display statistically significant increasing trends ($p < 0.05$) since 1950 regardless of the storm identification approach (Table 3). Likewise, a significant increasing trend is found for the winter $ST_p$, while no statistically significant trend is identified for $SH_s$ and storm counts determined using the storm identification algorithm (Table 3). For the storm datasets covering the last 40 years, none of the trends for the various parameters are statistically significant, although these display a tendency for negative trends in duration, power and $ST_p^{98}$, and positive for the other storm metrics. The change in direction and statistical significance of the trends, when considering different analysis periods, results from the grouping of very energetic winters around 1990, which affects the linear trend estimation (Fig. 7).

The storminess trends determined using the different calibrated datasets display a general agreement, but there is a significant positive $SH_s$ trend (6.5 mm/yr, $p < 0.1$) according to the cCMEMS-40 dataset, while for cERA5-40 or cERA-70 there are no statistically significant trends for the same variable. In contrast to the winter $SH_s$, mean winter $H_s$ has a significant long-term (70-year) increasing trend (7 mm/yr, $p < 0.05$), while no statistically significant trends are present in the shorter, 40-year datasets (cERA5-40 and cCMEMS-40) (Table 4). The winter $T_p$ and $T_p^{98}$ trends are only significant and positive when considering the longer 70-year dataset and winter $H_s^{98}$ show contrasting not statistically significant magnitudes for the two different analysed periods.

Considering the temporal variability of the NAO as the dominant mode of climate variability in the NE Atlantic, from 1950 to 2020 the extended winter NAO shows both a significant positive linear long-term trend (Fig. 8A) and a positive correlation with winter storm parameters (Table 5). Negative NAO conditions are related to shorter cumulative storm duration and lower storm power, while positive NAO conditions are linked to more energetic winters in the Outer Hebrides (Fig. 8B, C, D). Winter storm counts, cumulative duration, and power are all strongly correlated with the NAO, regardless of the storm identification approach (Table 5). For the mean and extreme storm parameters ($SH_s$, $SH_s^{98}$, $ST_p$ and $ST_p^{98}$) correlation with the NAO is mostly

**Table 3** Winter storm trends in the Outer Hebrides

| | $\overline{SH_s}$(mm/yr) | $\overline{ST_p}$(ms/yr) | $ST_p^{98}$(ms/yr) | Counts (n/yr) | Duration (h/yr) | Power ($MWhm^{-1}$/yr) |
|---|---|---|---|---|---|---|
| cERA5-70 | | | | | | |
| POT | 1.77 | **9.22** | **10.44** | **0.13** | **3.03** | **1.43** |
| $Storm_{ID}$ | – 0.62 | **5.38** | <u>8.84</u> | 0.00 | **4.81** | **1.82** |
| cERA5-40 | | | | | | |
| POT | 0.38 | 1.68 | – 11.18 | – 0.05 | – 1.61 | – 0.86 |
| $Storm_{ID}$ | 3.32 | 3.93 | – 8.07 | 0.00 | – 2.85 | – 1.00 |
| cCMEMS-40 | | | | | | |
| POT | 2.97 | 0.54 | – 0.76 | 0.00 | – 1.23 | – 0.78 |
| $Storm_{ID}$ | <u>6.50</u> | 0.08 | – 0.21 | 0.00 | – 2.88 | – 0.87 |

Trends are based on different wave data (calibrated ERA5 and CMEMS reanalysis), analysis periods (40 and 70 years), and storm identification approaches (Storm identification algorithm ($Storm_{ID}$) and POT). Statistically significant trends for 0.05 and 0.1 significance levels are indicated in bold and underlined, respectively

**Table 4** Winter wave trends in the Outer Hebrides

| | $\overline{H_s}$(mm/yr) | $\overline{T_P}$(ms/yr) | $H_s^{98}$(mm/yr) | $T_P^{98}$(ms/yr) |
|---|---|---|---|---|
| cERA5-70 | **7** | **8.4** | 9.9 | **8.4** |
| cERA5-40 | – 3.2 | 5.7 | – 16.8 | – 0.9 |
| cCMEMS-40 | – 5.9 | 0.4 | – 13.7 | 3.7 |

Trends are based on different wave data (calibrated ERA5 and CMEMS reanalysis) and analysis period (40 and 70 years). Statistically significant trends for 0.05 and 0.1 significance levels are indicated in bold and underlined, respectively

weak and not statistically significant, while winter mean $H_s$ and $T_p$ are strongly correlated with the NAO ($R \cong 0.9$), reaffirming the role of the NAO as the overwhelming climatological control in interannual storm wave variability in the west of Scotland.

## 4 Discussion

### 4.1 Storm identification and characterisation

The identification of coastal storms can differ substantially according to the scope of analysis, and the choice of storm criteria, which is often arbitrary. This has been highlighted by Harley (2017) and Martzikos et al. (2021a), who reviewed the broad-scale application of statistical storm analyses and the accompanying challenges in defining a generalised storm identification approach. Both reviews concluded that ST, MSD, and ID are the most commonly used criteria to identify storms from $H_s$ records. There is a broad consensus that ST can be determined based on the 95th percentile of the $H_s$ time series, while a MSD of either 6 or 12 h appropriately represents the minimum duration of a coastal storm event. However, the meteorological independence between consecutive storms is poorly defined.

Independence duration can be determined based on the minimum or average time between distinct extratropical cyclones. As such, ID can display high variability according to location, ranging from 6 h on the Dutch coast (Li et al. 2014) to 336 h in Durban, South Africa (Corbella and Stretch 2012). For western Europe, Priestley et al. (2017a, b) reported that during the exceptional 2013/14 winter season, on average, one intense extratropical cyclone affected the British Isles every 60 h. Such intense cyclones are consistently associated with extreme waves in the North Atlantic (Gramcianinov et al. 2023a), supporting the use of 60 h as an upper bound for the minimum time window between storm wave events in the higher latitudes of the North Atlantic. Importantly, the higher ID estimated by the extremal index based on the Outer Hebrides winter wave datasets indicates values close to 60 h (Table 2). A separation of 2.5-days (i.e., 60 h) between independent extreme windstorms affecting western Europe in 1990 and 1999 was identified by Hanley and Caballero (2012). On the other hand, the lower bound of the ID determined with the extremal index for the Outer Hebrides wave datasets indicates a minimum separation of 48 h, which aligns with the declustering window applied by Barton et al. (2022) to study extreme precipitation events over Europe. This indicates that wintertime wave, wind and precipitation extremes in western Europe driven by synoptic-scale processes can be consistently individualised by considering ID of 2–2.5 days (48–60 h). Therefore, the statistical determination of ID using the extremal index to obtain independent coastal storms from wave time series provides results that are in agreement with the meteorological timescales of extratropical cyclones in the eastern North Atlantic.

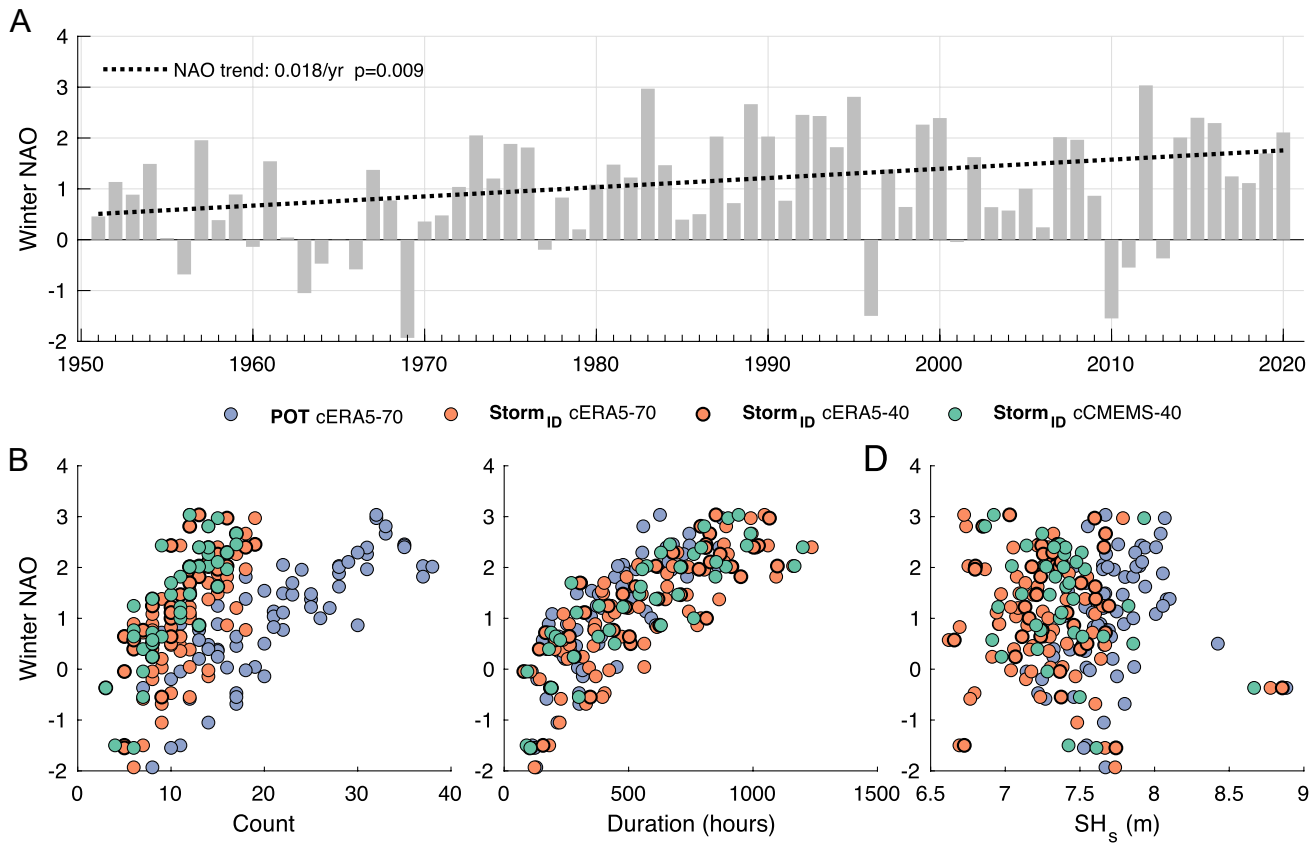


**Fig. 8** Temp or al variability of the extended winter NAO (**A**) and its correlation with winter storm counts (**B**), cumulative winter storm duration (**C**), and mean winter storm $H_s$ ($SH_s$) (**D**). Note that the storm parameters are based on different datasets and different storm identification approaches. The value of R and statistical significance of the correlations is listed in Table 5

**Table 5** Correlation between winter storm parameters and the NAO for different datasets and the two storm identification approaches

| | $\overline{SH_s}$ | $SH_s^{98}$ | $\overline{ST_P}$ | $ST_P^{98}$ | Count | Duration | Power |
|---|---|---|---|---|---|---|---|
| cERA5-70 | | | | | | | |
| POT | **0.29** | **0.27** | 0.23 | **0.32** | **0.81** | **0.79** | **0.77** |
| $Storm_{ID}$ | – 0.16 | 0.23 | 0.13 | **0.29** | **0.67** | **0.80** | **0.79** |
| cERA5-40 | | | | | | | |
| POT | 0.18 | 0.12 | – 0.15 | – 0.02 | **0.83** | **0.82** | **0.78** |
| $Storm_{ID}$ | – 0.15 | 0.09 | – 0.15 | – 0.02 | **0.81** | **0.83** | **0.8** |
| cCMEMS-40 | | | | | | | |
| POT | 0.12 | 0.09 | – 0.11 | 0.08 | **0.83** | **0.82** | **0.78** |
| $Storm_{ID}$ | – 0.28 | 0.03 | **– 0.35** | – 0.01 | **0.81** | **0.82** | **0.79** |

Statistically significant correlations for p-values below 0.05 and 0.1 are indicated in bold and underlined, respectively

Implementing ID in high-energy wave environments can lead to storms lasting for several weeks, with repeated periods where $H_s$ is below ST. The occurrence of serial cyclone clustering in the NE Atlantic and affecting the Outer Hebrides, causes rapid succession of winter storms, resulting in events characterised by multiple $H_s$ peaks with intermediate $H_s$ throughs (Fig. 5). Serial cyclone clustering is often the result of secondary cyclogenesis creating cyclone families that are constrained by large scale flows (jet stream and Rossby wave breaking) (Dacre and Pinto 2020). As each cyclone in the same family is not truly meteorologically independent, consecutive $H_s$ peaks can be considered as a single storm event, even though $H_s$ may fall below ST. In terms of coastal impacts, storms with aggregated $H_s$ peaks

can cause cumulative erosional impacts over extended periods, as there is not enought time for beach recovery in between $H_s$ peaks (Ferreira 2005; Splinter et al. 2014). However, it is also possible that rapidly succeeding storms are meteorologically unrelated events, possibly leading to a significant reduction in $H_s$ between storm events. This can be captured by implementing IT as proposed in the storm identification algorithm, which assumes that if waves reach $H_s$ values below the seasonal average, even if ID is not exceeded the following ST exceedance is considered an independent event. It is therefore strongly recommended that for statistical based climatological assessments appropriate statistically estimated ID values are considered and implemented to identify coastal storms that are associated with the driving storm meteorological mechanisms for a given coastal area.

The POT approach is a common method to define storms in coastal areas (e.g., Ciavola et al. 2014; Masselink et al. 2014, 2016; Flor-Blanco et al. 2021; Vieira et al. 2021; Celedón et al. 2022), probably due to its simplicity. However, the POT alone only defines peaks of ST exceedances without considering their independence or association with the relevant meteorological forcing. The inclusion of ID and IT can improve the ability to aggregate and distinguish exceedances of ST, improving the representation of the meteorological dynamics of coastal storm events (Harley 2017). This allows integrating knowledge of storm-driving meteorological processes and linking their changes to possible shifts in storm wave climatology (e.g., Lodise et al. 2022; Gramcianinov et al. 2023a). In addition, the subsequent storminess analysis is physically and statistically more robust than if performed with the POT approach alone. This is particularly important for assessing long-term trends and correlating storm parameters with large scale climatic indices such as the NAO to better understand and predict coastal hazards. Compared to the POT approach, the storm identification algorithm proposed in this work has the advantage of identifying storms that better represent natural extreme events especially in storm-dominated environments and, therefore, more correctly consider their potential consequences.

The characterisation of coastal storms is fundamental for understanding the potential impacts of storms and ultimately key to coastal risk reduction. For this purpose, wave reanalyses are an important tool, as they allow to extend observational time series in space and time, and the confidence in climatological analyses improves significantly with longer time series (e.g., Feser et al. 2020). In this work, buoy observations were compared with two wave reanalyses. ERA5, a global reanalysis, and CMEMS, a regional reanalysis with higher spatial resolution but lower temporal resolution. Both reanalyses showed very good performance for mean wave energy conditions, but underestimated observations of $H_s$ and $T_p$ during more energetic conditions. The systematic underestimation of extreme waves is a common limitation of several wave reanalyses, due to uncertainties in the wind forcing (Baordo et al. 2020). However, this can be improved by applying a number of calibration methods (Fanti et al. 2023). In the case of ERA5 and CMEMS, the calibration for the Outer Hebrides resulted in a significant improvement of reanalysis datasets (Fig. 3 and Fig. SM1). ERA5 was found to outperform CMEMS for storm conditions, resulting in improved agreement with the estimates of $H_s$ return periods obtained from buoy observations (Fig. 6), possibly due to the higher temporal resolution. Compared to its predecessor, ERA-Interim, the increase in temporal resolution from 6-h to a 1-h in ERA5, is reported to substantially improve the quality of the reanalysis product, including the representation of storm events (Hersbach et al. 2020). The very good agreement of the reanalysis datasets with the buoy observations allowed to extend the analysis period to the last 70 years and to obtain a robust assessment of the storm climatology in the Outer Hebrides, as well as to compare storm identification approaches in terms of climatological storm characterisation.

### 4.2 Long-term storm trends in the outer Hebrides

In the North Atlantic, there are inconsistencies in extreme wave trends between models, buoy observations and satellite data, particularly due to the use of different analysis periods (Bricheno et al. 2023). Based on a 7-member ensemble of different global wave products covering the period from 1980 to 2014, Erikson et al. (2022) found a decreasing but not statistically significant trend in the area of the Outer Hebrides for $H_s^{90}$ and high wave days, which are defined as the annual number of daily maximum $H_s$ exceeding 6 m. However, when considering a longer period between 1950 and 2008, there is a significant increasing trend in $H_s^{90}$ and $T_p^{90}$ for the west of Scotland (Dodet et al. 2010; Bromirski and Cayan 2015). According to the cERA5-70 dataset, winter $H_s$ and $H_s^{98}$ show a long-term significant increasing trend since 1950 with 13.6 and 8.3 mm/yr, respectively, which are consistent with the trend magnitudes reported by Castelle et al. (2018) for the study area. The cERA5-40 winter $SH_s$ determined using both storm identification approaches show no significant trend, and the cCMEMS-40 data shows an increasing trend but only at the lower confidence level ($p < 0.1$) (Table 3). The contrasting trends between the analysed periods (1950–2020 *versus* 1980–2020) demonstrate that linear trends depend strongly on the time frame of analysis due to multiannual and decadal variations in storm wave activity in the North Atlantic (Feser et al. 2020; Bricheno et al. 2023). Besides affecting linear trends, the strong variability of the wave climate in the North Atlantic challenges the selection of representative past reference periods for comparison with future wave climate projections or wave

energy resource assessments (e.g., Santo et al. 2015). This reinforces the need for long-term wave time series from reanalysis that have been carefully validated and calibrated against buoy observations.

The correlation of the interannual and multidecadal variability in storm activity in the west of Scotland with the NAO is well established (e.g., Dawson et al. 2004; Santo et al. 2015). The cluster of winter seasons with increased storm activity in the 1990s (Fig. 7) is mirrored by a prolonged and consistently positive phase of the NAO (Fig. 8). The 1990s are characterised by frequent and intense cyclones with anomalous extreme wind speeds and shortening of the North Atlantic storm track (Feser et al. 2020). The increased storm activity between 1980 and 2020 contrasts with the less intense winters between 1950 and 1980 (Fig. 7), which are associated with fewer and less intense positive NAO phases (Fig. 8) and are consistent with a reduced winter storm power for this region (Santo et al. 2015). Therefore, the winter storm variability in the Outer Hebrides evidences a strong climatic control and can be confidently linked to changes in the NAO.

The increase in winter storm activity is mainly determined by changes in storm duration and storm power, rather than by changes in winter storm counts (Fig. 7). It is important to note that the trend is unaffected by the method used to identify the storms, as this was applied consistently for all winters. While the number of winter storms determined by the POT approach shows similar patterns to the storm power calculated by the storm identification algorithm, it is possible that some spurious trends emerge from the POT approach, as this approach is still frequently used but lacks the robust independence between events obtained by the storm identification algorithm. Furthermore, both winter storm counts and duration determined by the storm identification algorithm are strongly correlated with the NAO index, which reinforces the confidence in the results obtained by this approach. The POT approach also captures the increasing trend in winter storm duration, but also an increasing trend in the number of winter storms, thus masking the increase in storm duration. This is a shortcoming of the POT approach, questioning its ability to adequately assess storminess variability and reinforcing the need for an improved storm identification as a basis for more robust storminess trend analysis. Bromirski and Cayan (2015) found no increasing trend in storm duration in the NE Atlantic and attributed an increasing trend in storm power to the higher frequency of winter storms. However, their analysis did not consider an independence duration to identify storm events, highlighting the different results that can be obtained by using different storm identification approaches. Importantly, Amaroche et al. (2022) used a storm identification approach similar to the storm identification algorithm proposed in this work and found that changes in storm intensity in the western Mediterranean are mainly driven by changes in storm duration.

Based on the storm identification algorithm, the winter of 2015 was the most energetic during the analysis period, coinciding with the longest winter storm duration (Fig. 7). Similarly, Loureiro and Cooper (2018) reported that this winter was the most energetic in the northwest of Ireland since 1950 due to exceptionally high $SH_s$. However, the POT approach does not identify the 2015 winter as the most energetic on record. Changes in storm duration have been associated with shifts in the extratropical cyclone track (Dolan et al. 1988), but recently longer storm duration has been more closely associated with the intensity of extratropical cyclones, which is controlled by the cyclone displacement speed (Gramcianinov et al. 2023a). For the North Atlantic region between 55°N and 70°N where the Outer Hebrides are located, Gramcianinov et al. (2023a) demonstrates that slower extratropical cyclone displacement speeds relative to its long-term climatology lead to longer storm duration. As storm duration is a fundamental parameter for determining the magnitude of storm impacts (e.g., Backstrom et al. 2022; Masselink et al. 2022), a robust assessment of regional changes in storm duration is crucial for coastal management. This can only be achieved by implementing robust statistical methods for identifying and characterising coastal storms.

## 5 Conclusions

A storm identification algorithm based on statistically defined criteria was developed to identify independent storms from $H_s$ records of the Outer Hebrides (Western Scotland), a storm-dominated, high wave energy coastal environment exposed to intense, frequent and rapidly succeeding winter storms. Storms are defined by a threshold based on the 95$^{th}$ percentile of $H_s$, but the independence of consecutive storm events is determined by a minimum duration between storm threshold exceedances or by reduction of $H_s$ to values below the winter average $H_s$. To avoid arbitrarily selecting the independence duration between consecutive storms, the proposed approach implements a minimum duration between storms based on the clustering tendency of the $H_s$ exceedances above the storm threshold determined by the extremal index. The criteria for storm independence determined by the statistical analysis are consistent with regional meteorological processes and timescales for extratropical cyclones in the eastern North Atlantic. Crucially, they allow the separation of independent winter storm events, even when they occur in rapid succession, but allow the aggregation of storm peaks associated with serially clustered extratropical cyclones, enabling an objective and robust storm characterisation. The identification algorithm is particularly suitable for high-energy, storm-dominated

coastal environments, such as those located along the main global extratropical storm tracks.

To assess its performance, the storm identification algorithm was compared to the common POT approach using 40 and 70-year-long calibrated wave reanalyses datasets for Western Scotland. Whilst the POT approach captures changes in extreme $H_s$, it can lead to spurious trends in storminess changes, as it lacks the robust independence between events that is achieved with the storm identification algorithm. The improved physical and statistical robustness of the storms identified by the storm algorithm is critical for understanding storm hazards and associated coastal risks. In addition, changes in the storm climatology determined using the storm identification algorithm can be linked to the driving meteorological dynamics, thereby improving the predictability of storm impacts.

The storminess analysis identified a significant increase in storm duration, contributing to an increasing trend in storm power in the west of Scotland. It also shows that multiannual and decadal variability in storm wave activity in the region is strongly related to the North Atlantic Oscillation. The results of this work highlight that regional assessments of storm climate variability, based on robust statistical approaches, are essential to complement basin and global-scale studies by providing deeper insights into changes in coastal storminess that are fundamental to coastal management planning.

**Supplementary Information** The online version contains supplementary material available at https://doi.org/10.1007/s00382-023-07017-w.

**Acknowledgements** Vincent Kümmerer receives funding for his Ph.D. through the Portuguese Foundation of Science and Technology (FCT) grant 2020.07497.DB. This work was supported by FCT, under the projects LA/P/00069/2020 (granted to the Associate Laboratory ARNET) and UID/00350/2020 CIMA. Access to the wave data from the Outer Hebrides wave buoy was kindly provided by CEFAS Wavenet and the reanalysis products from the ECMWF and the Copernicus Marine Service. Access to sea level pressure data was provided by the National Centre for Atmospheric Research for the sea level pressure data, and the storm tracks by was made available by John Lodise (https://github.com/jlodise/JGR2022_ExtratropicalCycloneTracker).

**Author contributions** Conceptualization: VK, VF, ÓF, CL; methodology: VK, VF, CL, ÓF; Formal analysis and investigation: VK, VF; Writing—original draft preparation: VK; writing—review and editing: CL, ÓF; Funding acquisition: VK; Supervision: CL, ÓF.

**Funding** Open access funding provided by FCT|FCCN (b-on). Vincent Kümmerer receives funding for his Ph.D. through the Portuguese Foundation of Science and Technology (FCT) grant 2020.07497.DB. This work was supported by FCT, under the projects LA/P/00069/2020 (granted to the Associate Laboratory ARNET) and UID/00350/2020 CIMA.

**Data availability** Access to the wave data from the Outer Hebrides wave buoy is provided by CEFAS Wavenet and the reanalysis products from the ECMWF and the Copernicus Marine Service. Access to sea level pressure data is provided by the National Centre for Atmospheric Research for the sea level pressure data, and the storm tracks was made available by John Lodise (https://github.com/jlodise/JGR2022_ExtratropicalCycloneTracker). The Matlab code of the storm identification algorithm will be available at https://github.com/vincentkuemmerer/.

## Declarations

**Conflict of interest** The authors declare that they have no conflict of interest/ competing interests.



## References

Almeida LP, Ferreira O, Vousdoukas MI, Dodet G (2011) Historical variation and trends in storminess along the Portuguese South Coast. Nat. Hazards Earth Syst. Sci. 11(9):2407–2417

Almeida LP, Vousdoukas MV, Ferreira Ó, Rodrigues BA, Matias A (2012) Thresholds for storm impacts on an exposed sandy coastal area in Southern Portugal. Geomorphology 143–144:3–12. https://doi.org/10.1016/j.geomorph.2011.04.047

Amarouche K, Akpınar A, Semedo A (2022) Wave storm events in the Western Mediterranean Sea over four decades. Ocean Model 170:101933. https://doi.org/10.1016/j.ocemod.2021.101933

Armaroli C, Ciavola P, Perini L, Calabrese L, Lorito S, Valentini A, Masina M (2012) Critical storm thresholds for significant morphological changes and damage along the Emilia-Romagna coastline, Italy. Geomorphology 143–144:34–51. https://doi.org/10.1016/j.geomorph.2011.09.006

Arns A, Wahl T, Haigh ID, Jensen J, Pattiaratchi C (2013) Estimating extreme water level probabilities: a comparison of the direct methods and recommendations for best practise. Coast Eng 81:51–66. https://doi.org/10.1016/j.coastaleng.2013.07.003

Backstrom JT, Loureiro C, Eulie DO (2022) Impacts of Hurricane Matthew on adjacent developed and undeveloped barrier islands in southeastern North Carolina. Regional Studies in Marine Science 53:102391. https://doi.org/10.1016/j.rsma.2022.102391

Baordo F, Clementi E, Iovino D, Masina S (2020) Intercomparison and assessement of wave models at global scale (Technical Notes No. TN0287). CMCC.

Barton Y, Giannakaki P, von Waldow H, Chevalier C, Pfahl S, Martius O (2016) Clustering of regional-scale extreme precipitation events in Southern Switzerland. Mon Weather Rev 144(1):347–369. https://doi.org/10.1175/MWR-D-15-0205.1

Barton Y, Rivoire P, Koh J, Kopp J, Martius O (2022) On the temporal clustering of European extreme precipitation events and its relationship to persistent and transient large-scale atmospheric drivers. Weather Clim Extremes 38:100518. https://doi.org/10.1016/j.wace.2022.100518

Bell B, Hersbach H, Simmons A, Berrisford P, Dahlgren P, Horányi A, Muñoz-Sabater J, Nicolas J, Radu R, Schepers D, Soci C, Villaume S, Bidlot J, Haimberger L, Woollen J, Buontempo C, Thépaut J (2021) The ERA5 global reanalysis: preliminary extension

to 1950. Q J R Meteorol Soc 147(741):4186–4227. https://doi.org/10.1002/qj.4174
Bricheno LM, Amies JD, Chowdhury P, Woolf D, Timmermans B (2023) Climate change impacts on storms and waves relevant to the UK and Ireland. MCCIP Sci Rev. https://doi.org/10.14465/2023.reu09.str
Bromirski PD, Cayan DR (2015) Wave power variability and trends across the North Atlantic influenced by decadal climate patterns: North Atlantic Decadal Wave Variability. Journal of Geophysical Research: Oceans 120(5):3419–3443. https://doi.org/10.1002/2014JC010440
Castelle B, Dodet G, Masselink G, Scott T (2017) A new climate index controlling winter wave activity along the Atlantic coast of Europe: the West Europe Pressure Anomaly. Geophys Res Lett. 44:1384–1392. https://doi.org/10.1002/2016GL072379
Castelle B, Dodet G, Masselink G, Scott T (2018) Increased winter-mean wave height, variability, and periodicity in the Northeast Atlantic over 1949–2017. Geophys Res Lett 45(8):3586–3596. https://doi.org/10.1002/2017GL076884
Castelle B, Marieu V, Bujan S, Splinter KD, Robinet A, Sénéchal N, Ferreira S (2015) Impact of the winter 2013–2014 series of severe Western Europe storms on a double-barred sandy coast: Beach and dune erosion and megacusp embayments. Geomorphology 238:135–148. https://doi.org/10.1016/j.geomorph.2015.03.006
Castelle B, Harley M (2020) Extreme events: impact and recovery. In: Sandy beach morphodynamics. https://www.sciencedirect.com/science/book/9780081029275. Accessed 05 Nov 2022
Celedón V, Del Río L, Ferreira Ó, Costas S, Plomaritis TA (2022) Identification of risk hotspots to storm events in a coastal region with high morphodynamic alongshore variability. Nat Hazards 115(1):461–488. https://doi.org/10.1007/s11069-022-05562-x
Ciavola P, Ferreira O, Dongeren AV, de Vries JVT, Armaroli C, Harley M (2014) Prediction of storm impacts on beach and dune systems. In: Quevauviller P (ed) Hydrometeorological hazards. Wiley, New York, pp 227–52. https://doi.org/10.1002/9781118629567.ch3d
Coles S (2001) An introduction to statistical modeling of extreme values. Springer, London. https://doi.org/10.1007/978-1-4471-3675-0
Corbella S, Stretch DD (2012) Multivariate return periods of sea storms for coastal erosion risk assessment. Nat Hazard 12(8):2699–2708. https://doi.org/10.5194/nhess-12-2699-2012
Dacre HF, Pinto JG (2020) Serial clustering of extratropical cyclones: A review of where, when and why it occurs. Npj Clim Atmos Sci 3(1):48. https://doi.org/10.1038/s41612-020-00152-9
Dawson A, Elliott L, Noone S, Hickey K, Holt T, Wadhams P, Foster I (2004) Historical storminess and climate 'see-saws' in the North Atlantic region. Mar Geol 210(1–4):247–259. https://doi.org/10.1016/j.margeo.2004.05.011
Dawson AG, Dawson S, Ritchie W (2007) Historical Climatology and coastal change associated with the 'Great Storm' of January 2005, South Uist and Benbecula Scottish outer hebrides. Scot Geograph J 123(2):135–149. https://doi.org/10.1080/14702540701623784
De Michele C, Salvadori G, Passoni G, Vezzoli R (2007) A multivariate model of sea storms using copulas. Coast Eng 54(10):734–751. https://doi.org/10.1016/j.coastaleng.2007.05.007
Del Río L, Plomaritis TA, Benavente J, Valladares M, Ribera P (2012) Establishing storm thresholds for the Spanish Gulf of Cádiz coast. Geomorphology 143–144:13–23. https://doi.org/10.1016/j.geomorph.2011.04.048
Dissanayake P, Brown J, Wisse P, Karunarathna H (2015) Effects of storm clustering on beach/dune evolution. Mar Geol 370:63–75. https://doi.org/10.1016/j.margeo.2015.10.010
Dodet G, Bertin X, Taborda R (2010) Wave climate variability in the North-East Atlantic Ocean over the last six decades. Ocean Model 31(3–4):120–131. https://doi.org/10.1016/j.ocemod.2009.10.010
Dolan R, Lin H, Hayden B (1988) Mid-Atlantic Coastal Storms. J Coastal Res 4(3):417–433
Erikson L, Morim J, Hemer M, Young I, Wang XL, Mentaschi L, Mori N, Semedo A, Stopa J, Grigorieva V, Gulev S, Aarnes O, Bidlot J-R, Breivik Ø, Bricheno L, Shimura T, Menendez M, Markina M, Sharmar V, Webb A (2022) Global ocean wave fields show consistent regional trends between 1980 and 2014 in a multi-product ensemble. Commun Earth Environ. 3(1):320. https://doi.org/10.1038/s43247-022-00654-9
Fanti V, Ferreira Ó, Kümmerer V, Loureiro C (2023) Improved estimates of extreme wave conditions in coastal areas from calibrated global reanalyses. Commun Earth Environ 4(1):151. https://doi.org/10.1038/s43247-023-00819-0
Fawcett L, Walshaw D (2008) Bayesian inference for clustered extremes. Extremes 11(3):217–233. https://doi.org/10.1007/s10687-007-0054-y
Ferreira JA, Guedes Soares C (1998) An application of the peaks over threshold method to predict extremes of significant wave height. J Offshore Mech Arct Eng 120(3):165–176. https://doi.org/10.1115/1.2829537
Ferreira O (2005) Storm groups versus extreme single storms: predicted erosion and management consequences. J Coastal Res SI(42):221–227
Ferro CAT, Segers J (2003) Inference for clusters of extreme values: clusters of extreme values. J R Stat Soc Series B Stat Methodol 65(2):545–556. https://doi.org/10.1111/1467-9868.00401
Feser F, Krueger O, Woth K, van Garderen L (2020) North Atlantic winter storm activity in modern reanalyses and pressure-based observations. J Clim 34(7):2411–2428. https://doi.org/10.1175/JCLI-D-20-0529.1
Flor-Blanco G, Alcántara-Carrió J, Jackson DWT, Flor G, Flores-Soriano C (2021) Coastal erosion in NW Spain: recent patterns under extreme storm wave events. Geomorphology 387:107767. https://doi.org/10.1016/j.geomorph.2021.107767
Garnier E, Ciavola P, Spencer T, Ferreira O, Armaroli C, McIvor A (2018) Historical analysis of storm events: case studies in France, England, Portugal and Italy. Coast Eng 134:10–23. https://doi.org/10.1016/j.coastaleng.2017.06.014
Gramcianinov CB, de Camargo R, Campos RM, Guedes Soares C, da Silva Dias PL (2023a) Impact of extratropical cyclone intensity and speed on the extreme wave trends in the Atlantic Ocean. Clim Dyn 60(5–6):1447–1466. https://doi.org/10.1007/s00382-022-06390-2
Gramcianinov CB, Staneva J, De Camargo R, Da Silva Dias PL (2023b) Changes in extreme wave events in the southwestern South Atlantic Ocean. Ocean Dyn 73(11):663–678. https://doi.org/10.1007/s10236-023-01575-7
Haigh ID, Wadey MP, Wahl T, Ozsoy O, Nicholls RJ, Brown JM, Horsburgh K, Gouldby B (2016) Spatial and temporal analysis of extreme sea level and storm surge events around the coastline of the UK. Scientific Data 3(1):160107. https://doi.org/10.1038/sdata.2016.107
Hall TM, Kossin JP (2019) Hurricane stalling along the North American coast and implications for rainfall. Npj Clim Atmos Sci 2(1):17. https://doi.org/10.1038/s41612-019-0074-8
Hanley J, Caballero R (2012) The role of large-scale atmospheric flow and Rossby wave breaking in the evolution of extreme windstorms over Europe: EXTREME EUROPEAN STORMS. Geophys Res Lett. https://doi.org/10.1029/2012GL053408
Harley MD (2017) Coastal storm definition. Coastal storms: processes and impacts. John Wiley and Sons Inc., New York, pp 1–22
Harley MD, Turner IL, Kinsela MA, Middleton JH, Mumford PJ, Splinter KD, Phillips MS, Simmons JA, Hanslow DJ, Short AD (2017) Extreme coastal erosion enhanced by anomalous extratropical storm wave direction. Sci Rep 7(1):6033. https://doi.org/10.1038/s41598-017-05792-1
Hersbach H, Bell B, Berrisford P, Hirahara S, Horányi A, Muñoz-Sabater J, Nicolas J, Peubey C, Radu R, Schepers D, Simmons

A, Soci C, Abdalla S, Abellan X, Balsamo G, Bechtold P, Biavati G, Bidlot J, Bonavita M, Thépaut J (2020) The ERA5 global reanalysis. Quart J R Meteorol Soc 146(730):1999–2049. https://doi.org/10.1002/qj.3803

Hochet A, Dodet G, Ardhuin F, Hemer M, Young I (2021) Sea state decadal variability in the North Atlantic: a review. Climate 9(12):173. https://doi.org/10.3390/cli9120173

Hurrell JW (1995) Decadal trends in the North Atlantic oscillation: regional temperatures and precipitation. Science 269(5224):676–679. https://doi.org/10.1126/science.269.5224.676

Li F, van Gelder PHAJM, Ranasinghe R, Callaghan DP, Jongejan RB (2014) Probabilistic modelling of extreme storms along the Dutch coast. Coast Eng 86:1–13. https://doi.org/10.1016/j.coastaleng.2013.12.009

Lobeto H, Menendez M, Losada IJ (2021) Future behavior of wind wave extremes due to climate change. Sci Rep 11(1):7869. https://doi.org/10.1038/s41598-021-86524-4

Lodise J, Merrifield S, Collins C, Rogowski P, Behrens J, Terrill E (2022) Global climatology of extratropical cyclones from a new tracking approach and associated wave heights from satellite radar altimeter. J Geophys Res Oceans. https://doi.org/10.1029/2022JC018925

Lopatoukhin LJ, Rozhkov VA, Ryabinin VE, Swail VR, Boukhanovsky AV, Degtyarev AB (2000) Estimation of extreme wind wave heights (WMO/TD-No. 1041 No. 9; JCOMM Technical Report No. 9, p. 70). https://repository.oceanbestpractices.org/bitstream/handle/11329/85/TR09.pdf?sequence=1. Accessed 05 Nov 2022

Loureiro C, Cooper JAG (2018) Temporal variability in winter wave conditions and storminess in the northwest of Ireland. Irish Geogr. https://doi.org/10.2014/igj.v51i2.1369

Loureiro C, Ferreira Ó, Cooper JAG (2012) Geologically constrained morphological variability and boundary effects on embayed beaches. Mar Geol 329–331:1–15. https://doi.org/10.1016/j.margeo.2012.09.010

Mailier PJ, Stephenson DB, Ferro CAT, Hodges KI (2006) Serial clustering of extratropical cyclones. Mon Weather Rev 134(8):2224–2240. https://doi.org/10.1175/MWR3160.1

Martzikos NT, Prinos PE, Memos CD, Tsoukala VK (2021a) Key research issues of coastal storm analysis. Ocean Coast Manag 199:105389. https://doi.org/10.1016/j.ocecoaman.2020.105389

Martzikos NT, Prinos PE, Memos CD, Tsoukala VK (2021b) Statistical analysis of mediterranean coastal storms. Oceanologia 63(1):133–148. https://doi.org/10.1016/j.oceano.2020.11.001

Masselink G, Austin M, Scott T, Poate T, Russell P (2014) Role of wave forcing, storms and NAO in outer bar dynamics on a high-energy, macro-tidal beach. Geomorphology 226:76–93. https://doi.org/10.1016/j.geomorph.2014.07.025

Masselink G, Castelle B, Scott T, Dodet G, Suanez S, Jackson D, Floc'h, F. (2016) Extreme wave activity during 2013/2014 winter and morphological impacts along the Atlantic coast of Europe. Geophys Res Lett 43(5):2135–2143. https://doi.org/10.1002/2015GL067492

Masselink G, Brooks S, Poate T, Stokes C, Scott T (2022) Coastal dune dynamics in embayed settings with sea-level rise—examples from the exposed and macrotidal north coast of SW England. Mar Geol 450:106853. https://doi.org/10.1016/j.margeo.2022.106853

Melet A, Meyssignac B, Almar R, Le Cozannet G (2018) Under-estimated wave contribution to coastal sea-level rise. Nat Clim Chang 8(3):234–239. https://doi.org/10.1038/s41558-018-0088-y

Mendoza ET, Jimenez JA, Mateo J (2011) A coastal storms intensity scale for the Catalan sea (NW Mediterranean). Nat Hazard 11(9):2453–2462. https://doi.org/10.5194/nhess-11-2453-2011

Mendoza ET, Trejo-Rangel MA, Salles P, Appendini CM, Lopez-Gonzalez J, Torres-Freyermuth A (2013) Storm characterisation and coastal hazards in the Yucatan Peninsula. J Coastal Res 65:790–795. https://doi.org/10.2112/SI65-134.1

Morim J, Vitousek S, Hemer M, Reguero B, Erikson L, Casas-Prat M, Wang XL, Semedo A, Mori N, Shimura T, Mentaschi L, Timmermans B (2021) Global-scale changes to extreme ocean wave events due to anthropogenic warming. Environ Res Lett 16(7):074056. https://doi.org/10.1088/1748-9326/ac1013

Neill SP, Vögler A, Goward-Brown AJ, Baston S, Lewis MJ, Gillibrand PA, Waldman S, Woolf DK (2017) The wave and tidal resource of Scotland. Renewable Energy 114:3–17. https://doi.org/10.1016/j.renene.2017.03.027

Neumann B, Vafeidis AT, Zimmermann J, Nicholls RJ (2015) Future coastal population growth and exposure to sea-level rise and coastal flooding—a global assessment. PLoS ONE 10(3):e0118571. https://doi.org/10.1371/journal.pone.0118571

Oikonomou CLG, Gradowski M, Kalogeri C, Sarmento AJNA (2020) On defining storm intervals: extreme wave analysis using extremal index inferencing of the run length parameter. Ocean Eng 217:107988. https://doi.org/10.1016/j.oceaneng.2020.107988

Pinto JG, Gómara I, Masato G, Dacre HF, Woollings T, Caballero R (2014) Large-scale dynamics associated with clustering of extratropical cyclones affecting Western Europe. Journal of Geophysical Research: Atmospheres 119(24):13704–13719. https://doi.org/10.1002/2014JD022305

Plomaritis TA, Benavente J, Laiz I, Del Río L (2015) Variability in storm climate along the Gulf of Cadiz: The role of large scale atmospheric forcing and implications to coastal hazards. Clim Dyn 45(9–10):2499–2514. https://doi.org/10.1007/s00382-015-2486-4

Priestley MDK, Dacre HF, Shaffrey LC, Schemm S, Pinto JG (2020) The role of secondary cyclones and cyclone families for the North Atlantic storm track and clustering over western Europe. Abstract Quart J Royal Meteorol Soc 146(728):1184–1205. https://doi.org/10.1002/qj.3733

Priestley MDK, Pinto JG, Dacre HF, Shaffrey LC (2017a) Rossby wave breaking, the upper level jet, and serial clustering of extratropical cyclones in western Europe: WESTERN EUROPE CLUSTERING DYNAMICS. Geophys Res Lett 44(1):514–521. https://doi.org/10.1002/2016GL071277

Priestley MDK, Pinto JG, Dacre HF, Shaffrey LC (2017b) The role of cyclone clustering during the stormy winter of 2013/2014. Weather 72(7):187–192. https://doi.org/10.1002/wea.3025

Ramsay DL, Brampton AH (2000) Coastal cells in Scotland: Cells 8 & 9—The Western Isles. Scottish Natural Heritage Research, Survey and Monitoring Report No 150. p. 120. https://www.dynamiccoast.com/files/Ramsay_Brampton_Cell_0809.pdf

Santo H, Taylor PH, Woollings T, Poulson S (2015) Decadal wave power variability in the North-East Atlantic and North Sea: WAVE POWER VARIABILITY. Geophys Res Lett 42(12):4956–4963. https://doi.org/10.1002/2015GL064488

Scott T, McCarroll RJ, Masselink G, Castelle B, Dodet G, Saulter A, Scaife AA, Dunstone N (2021) Role of atmospheric indices in describing inshore directional wave climate in the United Kingdom and Ireland. Earth's Future. https://doi.org/10.1029/2020EF001625

Senechal N, Coco G, Castelle B, Marieu V (2015) Storm impact on the seasonal shoreline dynamics of a meso- to macrotidal open sandy beach (Biscarrosse, France). Geomorphology 228:448–461. https://doi.org/10.1016/j.geomorph.2014.09.025

Sénéchal N, Castelle B, Bryan K (2017) Storm clustering and beach response. Coastal storms: processes and impacts. John Wiley and Sons, Inc, New York, pp 151–174

Serafin KA, Ruggiero P, Barnard PL, Stockdon HF (2019) The influence of shelf bathymetry and beach topography on extreme total water levels: Linking large-scale changes of the wave climate to local coastal hazards. Coast Eng 150:1–17. https://doi.org/10.1016/j.coastaleng.2019.03.012

Sharmar VD, Markina MYu, Gulev SK (2021) Global ocean wind-wave model hindcasts forced by different reanalyzes: a comparative

assessment. J Geophys Res Oceans 126(1):e2020JC016710. https://doi.org/10.1029/2020JC016710
Short AD (1999) Global variation in beach systems. Handbook of beach and shoreface morphodynamics. John Wiley and Sons, Inc, New York, pp 21–35
Smith RL, Weissman I (1994) Estimating the extremal index. J Roy Stat Soc: Ser B (methodol) 56(3):515–528. https://doi.org/10.1111/j.2517-6161.1994.tb01997.x
Smith AM, Mather AA, Bundy SC, Cooper JAG, Guastella LA, Ramsay PJ, Theron A (2010) Contrasting styles of swell-driven coastal erosion: Examples from KwaZulu-Natal. South Africa Geological Magazine 147(6):940–953. https://doi.org/10.1017/S0016756810000361
Splinter KD, Carley JT, Golshani A, Tomlinson R (2014) A relationship to describe the cumulative impact of storm clusters on beach erosion. Coast Eng 83:49–55. https://doi.org/10.1016/j.coastaleng.2013.10.001
Timmermans BW, Gommenginger CP, Dodet G, Bidlot J-R (2020) Global wave height trends and variability from new multimission satellite altimeter products, reanalyses, and wave buoys. Geophysl Res Lett. https://doi.org/10.1029/2019GL086880
Vieira BFV, Pinho JLS, Barros JAO (2021) Extreme wave value analysis under uncertainty of climate change scenarios off Iberian Peninsula coast. Ocean Eng 229:109018. https://doi.org/10.1016/j.oceaneng.2021.109018
Weisse R, Günther H (2007) Wave climate and long-term changes for the Southern North Sea obtained from a high-resolution hindcast 1958–2002. Ocean Dyn 57(3):161–172. https://doi.org/10.1007/s10236-006-0094-x
Wojtysiak K, Herman A, Moskalik M (2018) Wind wave climate of west Spitsbergen: seasonal variability and extreme events. Oceanologia 60(3):331–343. https://doi.org/10.1016/j.oceano.2018.01.002
Young IR, Ribal A (2019) Multiplatform evaluation of global trends in wind speed and wave height. Science 364(6440):548–552. https://doi.org/10.1126/science.aav9527